Expert Systems With Applications 213 (2023) 119228

Contents lists available at ScienceDirect

Expert Systems With Applications

journal homepage: www.elsevier.com/locate/eswa

A bi-objective green vehicle routing problem with a mixed fleet of conventional and electric trucks: Considering charging power and density of stations

Afsane Amiri[a], Saman Hassanzadeh Amin[a,*,1], Hossein Zolfagharinia[b]

[a] Department of Mechanical and Industrial Engineering, Toronto Metropolitan University, ON, Canada
[b] Ted Rogers School of Management, Toronto Metropolitan University, ON, Canada

ARTICLE INFO

Keywords:
Vehicle Routing Problem
Heavy-duty Electric Trucks
GHG Emissions
Bi-objective Programming

ABSTRACT

This paper considers a Green Vehicle Routing Problem (GVRP), which includes heavy-duty electric and conventional trucks. We develop a new bi-objective programming model defined on a set of vertices, including a depot, a group of customers, and a set of charging stations. The first objective function is the minimization of the total cost of transportation. To meet the growing environmental concerns, we also consider a second objective function which minimizes total Greenhouse Gas (GHG) emissions. To solve the bi-objective problem, we integrate three multi-objective solution methods (i.e., weighted-sum, ε-constraint, and hybrid methods) with the Adaptive Large Neighborhood Search (ALNS). We thereby generate a set of instances based on real-world locations in the Greater Toronto Area (GTA) and some parts of Ontario in Canada. These instances are then solved by applying the proposed solution methods. The obtained numerical results from the designed experiments revealed that by enhancing the charging power from 90 kW to 350 kW, transportation costs could decrease by up to 5 %. In addition, by doubling the number of stations in the same service area, delivery companies could lower their transportation costs by 2 %. Furthermore, a slight increase (less than 3 %) in transportation costs leads to a remarkable reduction (more than 18 %) in GHG emissions.

1. Introduction

Based on the Paris Agreement of 2016, Canada should reduce its GHG emissions by 30 % by 2030 (Pan-Canadian Framework on Clean Growth and Climate Change, 2016). However, the Government of Canada (2021a) reported that the country’s transportation sector, specifically, was responsible for a 54 % increase in GHG emissions from 1990 to 2019. Moreover, heavy-duty freight trucks contributed the majority of this emissions growth in Canada – approximately 70 % (Government of Canada, 2021a). Regarding this information, heavy-duty truck electrification may have a significant impact on reducing GHG emissions.

In recent years, a rapid inclination towards utilizing Electric Vehicles (EVs) has been witnessed. Governments, manufacturers, companies, and individuals are encouraged to use EVs, especially for reducing GHG emissions and decreasing fuel expenses. The existing literature has thus far mainly examined EV transportation problems for passenger cars (e.g., Pelletier et al., 2016), light and medium-duty trucks (e.g., Macrina et al., 2019a; Li et al., 2020), or electric buses (e.g., Hulagu et al., 2019). Additionally, several authors have focused on solution approaches and solving the problem for benchmark instances rather than real-world cases (e.g., Bruglieri et al., 2015; Koç and Karaoglan, 2016; Leggieri and Haouari, 2017). While there have been remarkable achievements in developing electric passenger cars and light-duty electric vans (Pelletier et al., 2016) heavy-duty all-electric trucks still face some obstacles to mass production. Such limitations include the short range of travel, high purchasing price, long recharging time, and lack of charging infrastructures (Capuder et al., 2020).

As mentioned above and based on a comprehensive report on commercial electric trucks published by the North America Council for Freight Efficiency (NACFE), heavy-duty electric trucks are currently best-suited for shorter distances and urban areas. The report indicates that diesel trucks will not be replaced entirely soon but will be substituted by electric trucks in the long term (Guidance Report: Viable

* Corresponding author.
E-mail addresses: afsane.amiri@ryerson.ca (A. Amiri), saman.amin@ryerson.ca (S.H. Amin), h.zolfagharinia@ryerson.ca (H. Zolfagharinia).
[1] ORCID: 0000-0001-6173-7530.

https://doi.org/10.1016/j.eswa.2022.119228
Received 23 April 2022; Received in revised form 3 November 2022; Accepted 3 November 2022
Available online 9 November 2022
0957-4174/

Class 7/8 Electric, 2019). Heavy-duty electric trucks are gradually finding their way to the market, and more EVs will be used shortly. Based on a recently published report by the Government of Canada (2021b), the government will accelerate the transition from heavy-duty trucks to non-zero emission vehicles by investing in the production of heavy-duty trucks. The Canadian government has also committed to supporting the development of charging infrastructures. Furthermore, according to the CALSTART (2020), only four models of heavy-duty electric trucks are available now in North America from three manufacturers, including BYD, Lion, and Meritor. Eleven models are also estimated to be produced by nine automakers by the end of 2022. Large companies such as UPS, Pepsi, DHL, and Walmart have already ordered some of these models (Green Car Reports, 2017). For such reason, it would be worthwhile to evaluate the effectiveness of using electric trucks in addition to conventional trucks in planning delivery routes. Based on these ongoing trends, the idea of including heavy-duty electric trucks in routing problems for delivery purposes is the focus of this paper. As such, in this study, the following research questions are considered:

a. What are the impacts of using heavy-duty mixed-fleet trucks for short-haul distances?

b. What are the impacts of some important factors (e.g., service area, charging power, and density of the stations) on the routing problem, including EVs?

c. What are the trade-offs between transportation costs and emissions in a mixed-fleet routing problem?

To investigate the problem and provide practical managerial insights, the design of experiments in this paper is inspired by parts of Walmart's distribution system in southern Ontario. The parameters related to heavy-duty electric trucks and charging stations are incorporated based on the currently available data. We examine the routing problem for heterogeneous heavy-duty trucks (including diesel and electric vehicles for short-haul transportation) for Walmart Canada in the GTA and surrounding areas up to 100 km. The problem is solved for a set of vertices comprising a depot, a set of customers, and a set of potential charging stations based on two objectives: minimizing transportation costs and minimizing fuel consumption (GHG emissions). To the best of our knowledge, considering these two objectives simultaneously and performing trade-off analyses for GHG emissions and transportation costs are new in the literature. These analyses provide insights for decision-makers about the trade-off between transportation costs and GHG emissions. The transportation costs computed by the model's first objective are comprehensive and include all the cost components of the routing problem. Three multi-objective techniques, including weighted-sum, ε-constraint, and hybrid methods, are integrated with Adaptive Large Neighborhood Search (ALNS) to solve the bi-objective problem. The removal and insertion operators for the Adaptive ALNS algorithm are designed for the proposed problem of solving large-size instances. In addition, the design of the experiments is inspired by real-world locations for short-haul transportation delivery problems and real-world parameters for heavy-duty electric trucks. Lastly, the impact of different important factors such as the service area, the density of stations, and charging power is analyzed, and managerial insights for delivery companies are provided. Hence, the main research contributions of this work are summarized as follows:

- Developing a new variation of the GVRP for a mixed-fleet of vehicles including electric and diesel heavy-duty trucks. This includes developing a new bi-objective programming model for the GVRP and computing GHG emissions for the diesel trucks and the overall transportation costs.
- Developing solution approaches by considering bi-objective solution methods and metaheuristic algorithms to solve the model.
- Applying the model for short-haul distances in Ontario, Canada considering real-world operational parameters for heavy-duty trucks.
- Offering managerial insights by analyzing the impact of three factors (i.e., service area, power of charge, and density of the stations) on transportation costs and emissions.

The remainder of this paper is organized as follows. The existing literature on Electric Vehicle Routing Problem (EVRP) and multi-objective Vehicle Routing Problem (VRP) is summarized in Section 2. Section 3 defines the bi-objective green vehicle routing problem for which the bi-objective mathematical model is provided in Section 4. Section 5 presents the proposed solution approaches. Lastly, the computational results are presented in Section 6, followed by concluding remarks in Section 7.

2. Literature review

The main goal of the EVRP is to solve the routing problem by considering a fleet of EVs and their limitations in range, duration of recharge, and scarcity of charging stations. Hence, considering these limitations, the EVRP has become a more complicated problem than the general VRP. We first review the EVRP literature in Section 2.1 to illustrate how other researchers have handled this complexity. However, since multi-objective problems need to be treated differently from single-objective problems, we also discuss VRPs with more than one objective function in Section 2.2.

2.1. EVRP

EVRP was first introduced by Conrad and Figliozzi (2011), who solved a routing problem for a capacitated VRP with time windows for a fleet. In their work, vehicles needed to be charged at customer nodes because of their limited range of travel. Erdoğan and Miller-Hooks (2012) introduced the green vehicle routing problem (GVRP) and considered Alternative Fuel Vehicles (AFV) as available vehicles of the problem. Felipe et al. (2014) and Schneider et al. (2014) presented the EVRP with load capacity and time windows in the same year with different approaches for formulating the mathematical model and solution methods. Most of the authors were inspired by the work of Schneider et al. (2014) in modeling their EVRP (Hiermann et al., 2016; Keskin and Çatay, 2018; Macrina et al., 2019b). Yang et al. (2021) developed a quadratic zero-one programming model to address an EVRP with pickup and delivery. They solved the problem by alternating the direction method of multipliers (ADMM) and augmented Lagrangian relaxation.

Moreover, the EVRP with a non-linear charging function was first modeled by Montoya et al. (2017). They showed that the charging curve changes linearly until 80 % of the battery capacity and then grows logarithmic. Froger et al. (2019) extended the formulation of Montoya et al. (2017) by replacing the node-based formulation with an arc-based formulation. They solved the problem by combining heuristic and exact methods. The works of Villegas et al. (2018), Zuo et al. (2019), Koç et al. (2019), Kullman et al. (2020), and Lee (2020) also considered non-linear charging functions.

The other and more comprehensive approach to the EVRP was presented by Keskin et al. (2019). They introduced an EVRP with soft time windows and wait times at the charging stations and solved the routing problem by calculating the time the vehicles may spend in the queues at the station. In addition, they considered a non-linear charging time function. Some papers in the domain of EVRP have considered a heterogeneous fleet, including electric and Conventional Vehicles (CV). Gonçalves et al. (2011) solved a VRP with pickup and delivery for a fleet of electric and conventional vehicles. Sassi et al. (2014) examined the VRP with a mixed fleet to reduce the number of vehicles and the cost of recharging and travel. They extended their work by developing new solution approaches for their previous model (Sassi et al., 2015a; Sassi et al., 2015b). Goeke and Schneider (2015) added an energy consumption model for EVs by combining speed, road profile, and load weight.

Similarly, Macrina et al. (2019b) defined an energy consumption model for both EVs and CVs by incorporating curb weight, speed, load, and gradients. Although these factors are essential for accurately calculating the energy consumption in EVs, to maintain the simplicity of the presented study, an average rate per distance is considered for the energy consumption rate. Vincent et al. (2021) solved another version of the mixed fleet vehicle routing problem by applying the ALNS algorithm. In addition, they considered partial recharge and fuel consumption rates in the problem under investigation. For further studies about the GVRP, readers may refer to a survey on the EVRP by Erdelić and Carić (2019) and a review of the GVRP by Asghari et al. (2020). Table 1 classifies the EVRP papers in terms of the main factors of the problem.

Table 1
A summary of the related EVRPs literature.

Reference	Time windows	Load capacity	Mixed-fleet	Charging function behavior	Partial recharge	Objective function (Minimization)	Solution methods
Conrad and Figliozzi (2011)					*	Acquisition cost, travel cost, recharging cost, time cost	Iterative route construction and improvement heuristic algorithm
Schneider et al. (2014)	*	*				Vehicle cost, travel cost	VNS and TS
Felipe et al. (2014)	*	*			*	Travel cost, recharging cost	Constructive and local search heuristics and SA
Sassi et al. (2014)	*	*	*		*	Acquisition cost, travel cost, recharging cost	Charging routing heuristic and a local search heuristic
Bruglieri et al. (2015)	*	*			*	Acquisition cost, travel cost, recharging cost, charging infrastructure cost	VNSB
Goeke and Schneider (2015)	*	*	*			Travel cost, recharging cost, time cost, fuel cost, battery cost	ALNS
Ding et al. (2015)	*	*			*	Travel cost	VNS and TS
Sassi et al. (2015a)	*	*	*		*	Acquisition cost, travel cost, recharging cost	ILS based on an LNS
Sassi et al. (2015b)	*	*	*		*	Acquisition cost, travel cost, recharging cost	ITS based on an LNS
Montoya et al. (2016)						Travel cost	MSH
Desaulniers et al. (2016)	*	*				Travel cost	Exact branch-price-and-cut algorithms
Koç and Karaoglan (2016)	*					Travel cost	SA heuristic and a branch-and-cut algorithm
Hiermann et al. (2016)	*	*	*			Acquisition cost, travel cost	A branch-and-price algorithm and ALNS
Montoya et al. (2017)				*	*	Time cost	Hybrid meta-heuristic
Froger et al. (2017)				*	*	Time cost	A route-first assemble-second meta-heuristic
Leggieri and Haouari (2017)	*	*				Travel cost	Exact algorithm (CPLEX 12.6.1.)
Villegas et al. (2018)	*		*	*	*	Acquisition cost, travel cost, recharging cost	GRASP
Keskin and Çatay (2018)	*	*			*	Acquisition cost, recharging cost	ALNS and exact algorithm
Zhang et al. (2018)		*				Energy Consumption	ACO
Macrina et al. (2019a)	*	*	*		*	Travel cost, recharging cost	ILS
Macrina et al. (2019b)	*	*	*		*	Travel cost, recharging cost	LNS
Froger et al. (2019)		*		*	*	Time cost	Heuristic and exact labeling algorithm
Keskin et al. (2019)	*	*			*	Energy cost, time cost, acquisition cost	ALNS
Zuo et al. (2019)	*	*		*		Acquisition cost, travel cost, recharging cost, time cost	Exact algorithm (CPLEX)
Koç et al. (2019)				*	*	Charging infrastructure cost, driver Cost	ALNS and exact algorithm
Eskandarpour et al. (2019)		*				Travel cost, CO_2 emissions	EMDLS
Ren et al. (2020)	*	*	*			Delay time, emissions	VNS
Kullman et al. (2020)				*	*	Travel cost	Exact and metaheuristic algorithms
Lee (2020)				*	*	Travel cost, recharging cost	Branch-and-price method
Yang et al. (2021)	*	*			*	Travel cost	Augmented Lagrangian relaxation and ADMM
Vincent et al. (2021)	*	*	*		*	Travel cost, Total pollution cost	ALNS
Current Study	*	*	*	*	*	Acquisition cost, travel cost, recharging cost, fuel consumption	ALNS-TS and ALNS-SA

NOTE. VNS = Variable Neighbourhood Search; TS = Tabu Search; SA = Simulated Annealing; VNSB = Variable Neighbourhood Search Branching; ALNS = Adaptive Large Neighbourhood Search; ILS = Iterated Local Search; LNS = Large Neighbourhood Search; ITS = Iterated Tabu Search; MSH = Multi-Space Sampling Heuristic; GRASP = Greedy Randomized Adaptive Search Procedure; ACO = Ant Colony Optimization; EMDLS = Enhanced Multi-Directional Local Search; ADMM = Alternating Direction Multiplier Method.

2.2. Multi-objective VRP

Different and usually conflicting objectives are considered in multi-objective programming (Caramia and Dell'Olmo, 2020). One of the most popular applications of this type of modeling is in the field of VRP. Generally, researchers minimize the total cost in the VRP by considering the time or distance of the constructed routes, while in most real-world cases, it is required to add objectives other than the cost. Several authors proposed a bi-objective VRP by minimizing the number of vehicles and the total cost of the routes (Alabas-Uslu, 2008; Braekers et al., 2011). Melián-Batista et al. (2014) defined cost and social objectives for the VRP. They minimized the total traveled distance and balanced the workload for each route. Guerriero et al. (2014) considered three objectives, including the minimization of total distances, maximization of customers' satisfaction, and minimization of the number of vehicles. Recently, Bula et al. (2019) presented a bi-objective VRP for transporting hazardous materials in which the total risk and the total cost of the tours are minimized.

Common solution approaches used in several multi-objective VRPs include evolutionary algorithms, GA, ant-colony, and particle swarm optimization. Garcia-Najera and Bullinaria (2011) utilized an evolutionary algorithm to solve a VRP with three objectives: minimizing the number of routes, the total distance, and the total time of travel. Ghoseiri and Ghannadpour (2010) solved a bi-objective VRP using goal programming and GA. Their goals were to minimize the number of vehicles and the total traveled distance. Zhang et al. (2019), on the other hand, maximized customers' satisfaction while minimizing transportation costs by applying hybrid ant-colony optimization. Finally, Dabiri et al. (2017) solved a bi-objective inventory routing problem by applying particle swarm optimization. Eskandarpour et al. (2019) proposed a bi-objective model for a mixed-fleet VRP and solved the model by using Enhanced Multi-Directional Local Search (EMDLS) which was based on the Large Neighborhood Search (LNS) algorithm. Their obtained results showed that their proposed algorithm can produce a wide range of Pareto solutions. The other bi-objective model for the mixed-fleet GVRP was presented by Ren et al. (2020). Their proposed bi-objective model minimized emissions and delay time simultaneously. They solved the proposed model using a variant of Variable Neighborhood Search (VNS) which employed a selection mechanism to find the Pareto solutions. In a recent study, Tirkolaee et al. (2022) solved a multi-objective sustainable waste collection routing problem by developing two different algorithms based on Simulated Annealing (SA) and invasive weed optimization. The objectives of the problem were minimizing the total cost, the total emissions, the workload of the drivers, and maximizing the hired drivers. In another study, Zarouk et al. (2022) integrated the chance-constraint and ε-constraint multi-objective solution approaches with GA and SA algorithms to solve a bi-objective routing and scheduling problem. The objectives of the problem were to minimize fuel consumption and the violations from time windows. While the authors did not consider electric vehicles in the routing problem, they solved it by considering a heterogeneous fleet of vehicles with different maximum load capacities.

For further studies, readers may refer to a review of multi-objective routing problems written by Zajac and Huber (2021). With regards to environmental concerns, Demir et al. (2014) developed the problem of pollution-routing by considering two objectives. The first goal of the problem was to minimize fuel consumption while the second was to decrease the total time of travel. The authors proposed a hybrid method which is a combination of weighted-sum and ε-constraint methods and incorporated this method with an ALNS to solve the routing problem. Demir et al. (2014) based their algorithm on the work of Ropke and Pisinger (2006) which demonstrated the effectiveness of the ALNS for the VRP.

3. Problem statement

Heavy-duty trucks in short-haul transportation usually travel longer distances than light-duty trucks and carry larger payloads. Hence, their contribution to pollution is more significant. Moreover, with the fast-approaching availability of heavy-duty electric trucks by 2022 and the fact that delivery companies that want to use EVs already have CVs in their fleet, it is necessary to solve the routing problem for a mixed-fleet of CVs and EVs considering real-world locations. For such reasons, it is essential to calculate and reduce the amount of GHG emissions which are released by heavy-duty diesel trucks. To address these concerns, we develop a bi-objective GVRP with a mixed-fleet of heavy-duty diesel and electric trucks for real-world locations.

The GVRP involves constructing optimal tours that start from the depot, visit all the customers, some of the charging stations, and return to the depot. The first objective of the problem is to minimize the total cost comprising of the recharging cost, acquisition cost, and travel cost, whereas the second objective is to minimize the fuel consumption for diesel trucks which results in reducing GHG emissions.

We consider two determining factors in the EVRP (i.e., waiting time at the stations and 80 % charge instead of full charge). In reality, the chargers may not be available immediately, and the vehicles must wait for a while. Based on a case study in a recent paper (Parastvand et al., 2020), we assume that the average daily waiting time is 12 min, it differs from 4 to 18 min in off-peak and peak hours, respectively. Other recent reports also indicate that by using new methods and technologies, the average waiting time at the stations can be as low as 10 to 12 min (Shukla et al., 2019; Schoenberg and Dressler, 2022).

Montoya et al. (2017) indicated that the charging curve is a linear function of time until 80 % of the battery capacity, and after that, it increases concavely. Since having a full charge takes a much longer time, it is assumed that all the vehicles are charged until 80 % of their battery capacities. This assumption makes the problem more reasonable in terms of the recharging time and reduces the complexity.

4. Mathematical model

The notations for the bi-objective mathematical model developed for solving a variant of the GVRP are defined in Table 2. Set $K = K_e \cup K_c$ includes all the available CVs and EVs. Set $N_{0,n+1} = \{0, 1, \cdots, n+1\}$ includes the departure depot $\{0\}$, customers D, charging stations F and their copies F', and the arrival depot $\{n+1\}$. Vehicle k is identified by an acquisition cost A^k, energy consumption per distance h^k, maximum load capacity Q^k, maximum capacity for recharging R^k, and the percent of charge (θ^k) when it leaves the departure depot. Each arc (i, j) has an associated distance d_{ij}, travel time t_{ij}, and the cost of traveling a_{ij}^k by vehicle k. Each customer i has a service time T_i, a time window $[e_i, l_i]$, and a demand p_i. In addition, the parameters related to station i are waiting time ω_i, recharging cost r_i, and recharging time g_i^k for vehicle k. Binary variable of x_{ij}^k is used to determine the arcs that are visited by vehicles, and the positive variable of u_i that keeps track of the arrival time at each vertex i. When vehicle k arrives at vertex i, the variables of q_{ij}^k and y_i^k represent the current amounts of load and energy level, respectively. Lastly, variable v_i^k corresponds to the amount of charge received by vehicle k at station i.

The first objective function of this model is to minimize the total cost of transportation. This cost consists of charging expenses, acquisition, and operating costs. Eq. (1) shows the first objective function (Z_1) that minimizes the four-part total cost. The first term calculates the recharging cost, while the second expression computes the charging cost at the depot. After finishing its journey, the vehicle arrives at the arrival depot with an amount of charge left in its battery. This amount is deducted from the initial charge to create a more accurate calculation of the initial charge cost. The next expression corresponds to the

Table 2
The notations of the mathematical model.

Sets	
K_e	Set of available EVs
K_c	Set of available CVs
K	Set of all available vehicles $K_e \cup K_c$
D	Set of customers
F	Set of charging stations
F'	Set of charging stations and their copies (stations may be visited more than once)
N	Set of customers, charging stations and their copies $D \cup F'$
N_0	Set of customers, departure depot, charging stations and their copies $D \cup 0 \cup F'$
N_{n+1}	Set of customers, arrival depot, charging stations and their copies $D \cup (n+1) \cup F'$
$N_{0,n+1}$	Set of customers, depots, charging stations and their copies $D \cup 0 \cup (n+1) \cup F'$
Parameters	
A^k	Acquisition cost for vehicle k
a_{ij}^k	Cost of traveling from vertex i to vertex j by vehicle k
d_{ij}	Distance between vertex i and vertex j
h^k	Energy consumption per distance by vehicle k
t_{ij}	Travel time from vertex i to vertex j
T_i	Service time for each customer i
ω_i	Waiting time at station i
$[e_i, l_i]$	The time window for vertex i
p_i	The demand of customer i
Q^k	The maximum capacity of vehicle k for load
r	Recharging costs at the depot
r_i	Recharging cost at station i
g_i^k	Recharging rate for vehicle k in station i
R^k	The battery capacity of vehicle k
θ^k	Percent of the initial charge of the battery when vehicle k leaves the departure depot
ξ	Fuel-to-air mass ratio
f	Engine friction factor
I	Engine speed
E	Engine displacement
m	The efficiency parameter for diesel engines
n	The heating value of typical diesel fuel
P	Engine power
P_t	Total tractive power required by the vehicle
P_e	Power related to running losses of the engine
W_T	Total weight of the vehicle
W_v	Curb weight
W_l	Payload
τ	The average acceleration of the vehicle
G	Gravitational constant
δ	Angle of road
C_a	Aerodynamic drag coefficient
C_r	Rolling resistance coefficient
A_v	The frontal area of the vehicle
ψ	A constant which converts *gram/s* to *litre/s*
ν	The average speed of the vehicle
Variables	
x_{ij}^k	1 if vehicle k travels arc *(i, j)*, 0 otherwise
u_i	Arrival time of vertex i
q_{ij}^k	The flow of load carried from vertex i to vertex j by vehicle k
y_i^k	The current energy level of vehicle k when arriving at vertex i
v_i^k	The amount of energy that vehicle k receives at station i

acquisition cost, including the procuring and labor costs (drivers' wage in Canada, which is about $23 per hour, is considered as the labor cost for an 8-hour shift in this paper (see, e.g., Nauvoo (2020)). The fourth term accounts for the operating cost along the route. The fuel costs of CVs are included in the operating costs, in addition to the maintenance costs. The maintenance costs for EVs are considered to be operating costs for this type of vehicle.

$$MinZ_1 = \sum_{k\in K_e}\sum_{i\in F'} r_i v_i^k + r\left(\sum_{k\in K_e}\left(\theta^k R^k \sum_{j\in N, i\neq j} x_{0j}^k - y_{n+1}^k\right)\right) + \sum_{k\in K}\sum_{j\in N} A^k x_{0j}^k + \sum_{k\in K}\sum_{i\in N_0}\sum_{j\in N_{n+1}, i\neq j} a_{ij}^k x_{ij}^k \tag{1}$$

The second objective function of this problem is to minimize GHG emissions released by diesel trucks. It is pertinent to mention that both objectives have the same level of importance. The GHG emissions are dependent directly on fuel consumption. The fuel consumption rate (R_f) is calculated based on the model which is introduced by Barth et al. (2005) and extended by Demir et al. (2014). See Eq. (2).

$$R_f = \frac{\xi(fIE + P/m)}{n} \tag{2}$$

In this equation, ξ denotes the fuel-to-air mass, and f stands for the engine friction factor. Engine speed and displacement are represented by I and E, respectively. Fuel-to-air mass is the mass ratio of air to the fuel that exists in the combustion process, while the engine displacement factor is measured based on the diameter and number of cylinders, and the distance that is traveled by pistons in the engine. m and n are efficiency parameters for diesel engines and the heating value of typical diesel fuel, respectively. P represents the engine power which is calculated based on Eq. (3) (Demir et al., 2014).

$$P = \frac{P_t}{o} + P_e \tag{3}$$

In this equation, P_t and P_e are the total tractive power required by the vehicle, and the power related to running losses of the engine, respectively. Tractive power is the force produced by the friction between the tires of the vehicle and the road. Parameter o represents vehicle drivetrain efficiency that determines the engine power losses through the drivetrain. P_t is obtained according to Eq. (4).

$$P_t = \frac{(W_T\tau + W_T G sin\delta + 0.5C_a\varphi A_v \nu + W_T G C_r cos\delta)\nu}{1000} \tag{4}$$

where W_T is the total weight of the vehicle, including the curb weight (W_v) and the load of the vehicle (W_l). τ denotes the acceleration ($\frac{m}{s^2}$). In addition, G is the gravitational constant, and δ represents the road angle. Aerodynamic drag and rolling resistance are shown by C_a and C_r coefficients, respectively. Besides, φ is the air density which is followed by the frontal area of the vehicle (A_v) in Eq. (4). ν is the speed of the vehicle. The effects of all these parameters on the fuel consumption model have been described comprehensively by Barth et al. (2005). According to Demir et al. (2014), $\lambda = \frac{\xi}{n\psi}$, $\rho = \frac{1}{1000mo}$, $\sigma = \tau + G sin\delta + G C_r cos\delta$ and $\epsilon = 0.5C_a\varphi A_v$ are set to simplify the equations. ψ is a constant which converts $\frac{gram}{s}$ to $\frac{litre}{s}$. Based on the previous equations, the fuel consumption rate is a function of the speed (ν) and the total weight (W_T) and is defined based on the following equation:

$$R_f(\nu, W_T) = \frac{\lambda(W_v\rho\sigma\nu + fIE + \epsilon\rho\nu^3 + \rho\sigma W_l\nu)d}{\nu} \tag{5}$$

The formula $\frac{d_{ij}}{t_{ij}}$ for obtaining speed (ν) is substituted in Eq. (5). The curb weight (W_v) impact on fuel consumption is considered in the first term of the function, while the load effect (q_{ij}^k) is calculated in the second term. Hence, the second objective function of the mathematical model (Z_2) is obtained according to Eq. (6).

$$MinZ_2 = \sum_{k\in K_c}\sum_{\forall i\in N_0}\sum_{j\in N_{n+1}, i\neq j}\left(W_v\rho\sigma_{ij}d_{ij} + fIEt_{ij} + \epsilon\rho d_{ij}(d_{ij}/t_{ij})^2\right)\lambda x_{ij}^k + \sum_{k\in K_c}\sum_{\forall i\in N_0}\sum_{j\in N_{n+1}, i\neq j}\rho\sigma_{ij}\lambda d_{ij} q_{ij}^k \tag{6}$$

Eqs. (7) – (11) are the routing constraints. Constraints set (7) guarantees that every customer is visited just once. By Constraints set (8), each station and its copies are restricted to be visited at most once. The connectivity of the tours is determined by Constraints set (9). Constraints set (10) ensures each vehicle must cover at most one tour. Constraints set (11) indicates that each tour starts from the departure depot and finishes at the arrival depot.

s.t.

$$\sum_{k\in K}\sum_{j\in N_{n+1},i\neq j} x_{ij}^k = 1 \qquad \forall i \in D, \tag{7}$$

$$\sum_{k\in K}\sum_{j\in D\cup n+1} x_{ij}^k \leq 1 \qquad \forall i \in F', \tag{8}$$

$$\sum_{i\in N_{n+1},i\neq j} x_{ji}^k - \sum_{i\in N_0,i\neq j} x_{ij}^k = 0 \qquad \forall k \in K, \forall j \in N, \tag{9}$$

$$\sum_{j\in N} x_{0j}^k \leq 1 \qquad \forall k \in K, \tag{10}$$

$$\sum_{j\in N_{n+1}} x_{0j}^k = \sum_{j\in N_0} x_{j(n+1)}^k \qquad \forall k \in K, \tag{11}$$

Eqs. (12) – (14) denote the time window constraints. Constraints set (12) forces that the arrival time for each customer must be within $[e_i, l_i]$ interval. Constraints set (13) guarantees that the start time for each node must be equal to or greater than the sum of the start time of the previous customer, its service time, and the travel time between these two nodes. Constraints set (14) ensures that if the previous node is a charging station, the start time of the node must be equal to or greater than the sum of the travel time between the nodes, the waiting time at the station, and the recharging time.

$$e_i \leq u_i \leq l_i \qquad \forall i \in N_{0,n+1}, \tag{12}$$

$$\begin{aligned} &u_i + (t_{ij} + T_i)x_{ij}^k - l_{n+1}\left(1 - x_{ij}^k\right) \leq u_j \\ &\quad \forall i \in D \cup 0, \forall j \in N_{n+1}, i \neq j, \forall k \in K, \end{aligned} \tag{13}$$

$$\begin{aligned} &u_i + (t_{ij} + \omega_i)x_{ij}^k + g_i^k v_i^k - \left(l_{n+1} + g_i^k R^k\right)\left(1 - x_{ij}^k\right) \leq u_j \\ &\quad \forall i \in F', \forall j \in N_{n+1}, \forall k \in K_e, \end{aligned} \tag{14}$$

Constraints set (15) denotes that the difference between the flow of the load that enters each vertex and the flow that leaves the same vertex is equal to its demand. Constraints sets (16) determine the maximum load capacity of the vehicles.

$$\sum_{j\in N_{n+1}} q_{ji}^k - \sum_{j\in N_{n+1}} q_{ij}^k = p_i \qquad \forall k \in K, \forall i \in N_0, \tag{15}$$

$$\begin{aligned} &p_j x_{ij}^k \leq q_{ij}^k \leq \left(Q^k - p_i\right)x_{ij}^k \\ &\forall k \in K, \forall i \in N_{0,n+1}, \forall j \in N_{n+1}, i \neq j, \end{aligned} \tag{16}$$

Eqs. (17) – (19) represent the energy constraints. Constraints set (17) shows that the available energy for each vehicle in each node must be equal to or less than the energy in the previous node minus the consumed energy between these nodes. Constraints set (18) implies the available energy when the previous node is a charging station. Constraints set (19) restricts the maximum charge received by the vehicle at the charging stations. Constraints set (20) determines the initial charge of the vehicle, and Constraints set (21) indicates that the associated variables for the energy level of the vehicle can have positive values if the vehicle starts a tour. This means that if a vehicle starts a tour and its associated energy level variable at departure depot {0} takes a value, the rest of the nodes on the tour until the arrival depot {n + 1} can have positive values.

$$\begin{aligned} &y_j^k \leq y_i^k - \left(h^k d_{ij}\right)x_{ij}^k + R^k\left(1 - x_{ij}^k\right) \\ &\forall i \in D, \forall j \in N_{n+1}, i \neq j, \forall k \in K_e, \end{aligned} \tag{17}$$

$$\begin{aligned} &y_j^k \leq v_i^k + y_i^k - \left(h^k d_{ij}\right)x_{ij}^k + R^k\left(1 - x_{ij}^k\right) \\ &\forall i \in F' \cup 0, \forall j \in N_{n+1}, \forall k \in K_e, \end{aligned} \tag{18}$$

$$0 \leq v_i^k + y_i^k \leq 0.8R^k \qquad \forall i \in F', \forall k \in K_e, \tag{19}$$

$$y_0^k = \theta^k R^k \sum_{j\in N_{n+1}} x_{0j}^k \qquad \forall k \in K_e, \tag{20}$$

$$y_j^k \leq \frac{1}{\theta^k} y_0^k \qquad \forall j \in N_{n+1} \forall k \in K_e, \tag{21}$$

Finally, the types of variables are determined by Constraints (22) – (26).

$$x_{ij}^k \in \{0,1\} \qquad \forall i \in N_0, \forall j \in N_{n+1}, i \neq j, \forall k \in K, \tag{22}$$

$$u_i \geq 0 \qquad \forall i \in N_{0,n+1}, \tag{23}$$

$$q_{ij}^k \geq 0 \qquad \forall i \in N_0, \forall j \in N_{n+1}, i \neq j, \forall k \in K, \tag{24}$$

$$y_i^k \geq 0 \qquad \forall i \in N_{0,n+1}, \forall k \in K_e, \tag{25}$$

$$v_i^k \geq 0 \qquad \forall i \in F', \forall k \in K_e, \tag{26}$$

5. Solution approaches

Since VRP is an NP-hard problem, commercial solvers cannot solve the model for large-size instances. Furthermore, the complexity of the proposed problem is more than the traditional VRP which leads us to utilize ALNS by using SA and TS approaches. In addition, three multi-objective methods are combined with the ALNS to solve the proposed bi-objective model. According to Table 1, neighborhood-search-based algorithms such as VNS and different variants of LNS are the most common approaches for solving EVRP (Macrina et al., 2019b; Keskin et al., 2019; Ren et al., 2020). Pisinger and Ropke (2007) illustrated that ALNS can produce solutions with high quality for different variants of the VRP for up to 1,000 customers. The presented GVRP covers different types of VRPs, including Capacitated VRP (CVRP) (Máximo and Nascimento, 2021), VRP with Time Windows (VRPTW) (Kyriakakis et al., 2022), and Heterogenous VRP (HVRP) (Máximo et al., 2022). Having a closer look at the literature, we can observe recent studies illustrated the efficiency of the ALNS algorithm in solving different types of VRPs. Some examples include the works of Chen et al. (2021), Voigt et al. (2022), and Friedrich and Elbert (2022), who utilized ALNS to solve VRPTW, CVRP, and HVRP, respectively. These promising results motivated us to adopt the ALNS algorithm for the problem under consideration. In addition, due to the structure of the problem (e.g., different tight constraints), searching multiple neighborhoods by applying ALNS can result in better diversification and intensification (Pisinger and Ropke, 2007). Other studies that consider a similar problem have also shown the effectiveness of ALNS in solving the EVRP (Kancharla and Ramadurai, 2018; Keskin et al., 2019; Vincent et al., 2021).

5.1. Metaheuristic algorithms

Since the proposed problem is an extension of the EVRP, it is an NP-hard problem. Due to the complexity of the EVRP, solvers such as CPLEX are unable to solve this problem for a large number of vertices. As observed from Table 1, most of the related literature used metaheuristic algorithms to solve the problem. Therefore, the metaheuristic algorithms have been developed in this paper to obtain qualified solutions in a reasonable computational time. We thereby use ALNS with different diversification approaches of SA and TS to solve the model with the first objective function (cost minimization). For solving the bi-objective model, we combine the ALNS algorithm with multi-objective solution approaches. The ALNS algorithm has been applied by several authors (e.g., Goeke and Schneider, 2015; Kancharla, and Ramadurai, 2018; Keskin et al., 2019) to find high-quality solutions for the EVRP. The presented ALNS algorithm first starts with an initial solution, then it improves the solution by applying different removal and insertion operators and attempts to avoid the local optima by using diversification approaches.

The main components of the proposed ALNS in this paper are explained in the following subsections.

5.1.1. Initial solution

The procedure of generating the initial solution begins by sorting the customers based on their latest time (l_i). The first route is constructed by starting from the departure depot to the customer with the minimum latest time and returning to the arrival depot. Then, the algorithm adds the customers from the sorted set to the route while maintaining the feasibility of the routes. The feasibility of the route is checked every time regarding the time window and the load capacity. If by adding the customer, the route will become infeasible, the insertion of the next customer is examined. When the first route has been completed, the next route is created by using a different type of vehicle. The first customer of the new route is the customer with the minimum latest time among all the unrouted remained customers. If an EV visits the route, the energy level is checked, and if there is not enough energy for continuing the journey, a charging station is added to the route. The procedure continues until all the customers are visited.

5.1.2. Removal and insertion operators

ALNS uses different removal and insertion operators to search the neighborhood of an initial solution. Nine removal operators for removing customers are applied for the developed problem including “Random”, “Worst Cost”, “Worst Time”, “Shaw”, “Proximity”, “Demand”, “Time-based”, “Customer Removal with Previous Station”, and “Customer Removal with Next Station”. The Worst Cost removal operator is modified based on our problem. All the customers are sorted based on the cost that they impose on the problem. The cost is calculated using the first objective function, and the operator removes β_1 percentage of the customers with the highest cost. The best value of β_1 is tuned by fixing all the other parameters and checking different values. The rest of the removal operators for customers and percentages are modified based on the characteristics of the presented problem (e.g., mixed-fleet of the vehicles). Customer Removal with Previous Station and Customer Removal with Next Station are only applied to routes traversed by EVs. The two removal operators, “Random” and “Greedy” are used to remove the routes in this study. The Greedy removal operator removes β_2 percentage of routes with the highest contribution to the first objective function. Four removal operators for deleting stations are applied that are called “Random”, “Worst Distance”, “Least Used”, and “Expensive”. The Least Used operator selects β_3 percentage of stations that have been visited less often by EVs. While the Expensive operator selects β_4 percentage of stations that impose the highest costs on the first objective function. Note that the station removal operators are only applied to the routes covered by EVs. There are three insertion operators for adding customers: “Greedy”, “Regret-2” and “Greedy with Noise”. The Greedy operator calculates the insertion costs for all the customers and adds β_5 percentage of the customers that impose the minimum costs to the first objective function. These customers should be added to the best location on the routes. If no feasible location has been found, a new route is generated. The remaining insertion operators have the same mechanism as those presented in the literature (Goeke and Schneider, 2015; Keskin and Çatay, 2016; Macrina et al., 2019b) but still need to be modified based on the features of the presented problem. Lastly, there are three operators for inserting stations: “Greedy”, “Greedy with Comparison” and “Best”. These operators are modified for our problem as follows:

- The maximum charge that the vehicle receives is 80 percent of their capacity.
- The partial recharge is considered where it is required.
- The cost of recharging is considered to determine the best station to visit.
- The operators are designed in a way that visiting two consecutive stations is not allowed.
- The time window constraint is checked whenever a station is considered for insertion.

It is worth mentioning that when each operator is applied, all the variables of the model, including the arrival time, the vehicle load, and the level of the battery for electric vehicles are updated. The time windows and capacity constraints are tested while applying the selected insertion operator. If these constraints are not violated, the new node is added to the feasible location. Otherwise, the possibility of adding a node to other locations is investigated and the node is added to the best feasible location. Regarding the energy level constraint, the battery level for electric vehicles at each node of the solution is checked after each iteration. If the energy level is negative, a Greedy Station Insertion operator is applied until all the energy level variables take positive values.

5.1.3. ALNS framework

After constructing the initial solution, the ALNS algorithm is applied. All the operators are chosen randomly in the first iteration and weights that are assigned to them are initially equal to 1. These weights are calculated in the subsequent iterations by Eq. (27) based on the operators’ performances.

$$W_o^i = W_o^{i-1}(1-\phi) + \phi \frac{S_o}{I_o} \tag{27}$$

W_o^i indicates the weight of operator o in iteration i, while ϕ is the roulette wheel parameter. The corresponding score for operator o is S_o, and the number of iterations that operator o has used is denoted by I_o. In the first iteration, all S_o s are equal to 0. If the best solution is improved, the algorithm adds σ_1 to all the scores associated with the applied operators. If the algorithm improved the current solution, the score for each operator is increased by σ_2. Finally, if the algorithm does not improve the current solution, but the new solution has been accepted, then the associated scores are updated by adding σ_3. According to the weights, the probability of choosing operator o is updated in iteration i based on Eq. (28). M is the number of operators for each type and W_j^i is the weight of operator j in iteration i.

$$Probability_o^i = \frac{W_o^i}{\sum_{j=1}^{M} W_j^i} \tag{28}$$

5.1.4. SA approach for diversification

To be consistent with the literature (see, e.g., Keskin and Çatay, 2016), we apply the SA algorithm to avoid local optimality. In each iteration, when the new solution is worse than the current one, a probability is calculated by Eq. (29). $Cost(NewSolution)$ indicates cost of the new solution, while $Cost(CurrentSolution)$ shows the cost of the current solution. The new solution is accepted if $Prob>\mu$. μ is a random number between $[0,1]$.

$$Prob = e^{\frac{-(Cost(NewSolution)-Cost(CurrentSolution))}{T}} \tag{29}$$

This probability is updated in each iteration based on T which is the temperature in the SA approach. T is set to an initial value at first, then multiplied by a cooling parameter ϵ $(0<\epsilon<1)$ in each iteration, thus $Prob$ value is updated in each iteration. To determine the initial value of T, a solution that worsens the initial solution by ϑ% is accepted with a 0.5 probability. All the parameters mentioned above are tuned based on the problem under investigation. To be consistent with the literature, the initial values of the parameters are adopted from Keskin and Çatay (2016), and 3 different values are considered for 8 instances from each set of problems. The pseudocode of the ALNS algorithm with SA approach (ALNS-SA) is shown in Algorithm 1. The number of iterations including *IterIn* and *IterOut* is set to 250 and 100, respectively. The initial values of the iterations are selected based on Keskin and Çatay (2016). Then, we performed a convergence analysis to set the number of iterations while considering a reasonable run time for the algorithm. After an initial investigation, the parameters with the most influence on the results are identified. Then, the parameter with the most impact is set to its best value and the best value for the next parameter is determined. Finally, the deviations from the best solution obtained from 8 runs are compared to choose the best values. This procedure goes on until all the parameters have been tuned.

Algorithm 1: ALNS-SA

Generate an initial solution and assign it to *Best Solution*;
Repeat
  Current Solution = *Best Solution*;
  Repeat
    Choose one of three types of removal operators (station, customer, route) based on $Probability_o^i$;
    Update I_o for the selected operator;
    if a station is removed **then**
      Select one of the insertion operators for the stations;
      Update I_o for the selected operator;
    else if a route is removed **then**
      Select one of the insertion operators for customers;
      Update I_o for the selected operator;
    else (if a customer is removed**)**
      Select one of the insertion operators for customers;
      Update I_o for the selected operator;
    end if
    if the solution is not feasible (the energy level is negative) **then**
      Apply Greedy Station Insertion operator;
    end if
    if $Cost(CurrentSolution) < Cost(BestSolution)$ **then**
      Update *Current Solution*;
      Update *Best Solution*;
      Update S_o s and W_o^i s for operators;
      Update $Probability_o^i$ s for operators;
    else if *Current Cost* has been improved from the previous iteration **then**
      Update *Current Solution*;
      Update S_o s and W_o^i s for operators;
      Update $Probability_o^i$ s for operators;
    else
      Prob is calculated;
      if $Prob > \mu$ **then**
        Update *Current Solution*;
        Update S_o s and W_o^i s for operators;
        Update $Probability_o^i$ s for operators;
      end if
    end if
  Until *IterIn* iterations are completed
Until *IterOut* iterations are completed
Output *Best;*

5.1.5. TS approach for diversification

In the TS approach, instead of SA, the algorithm tries not to go back to the neighborhoods searched recently to avoid local optimality. In this regard, the algorithm creates a tabu list from the attributes of the accepted solution in each iteration. In each iteration of the algorithm, the solution with the maximum reduction in the objective value is checked, and if its attributes are not in the tabu list, it will be accepted as the new solution. For each new solution, the added and removed customers are stored in the tabu list as attributes of that solution. The only exception happens when the solution has a smaller objective function value than the best objective function that has been found. The pseudocode of the ALNS-TS is presented in Algorithm 2. The effectiveness of the ALNS-SA and the ALNS-TS approaches for the developed problem will be investigated later in Section 6.4.

Algorithm 2: ALNS-TS

Generate an initial solution and assign it to *Best Solution*;
Repeat
  Current Solution = *Best Solution*;
  Repeat

(*continued on next column*)

(*continued*)

    Choose one of three types of removal operators (station, customer, route) based on $Probability_o^i$;
    Update I_o for the selected operator;
    if a station is removed **then**
      Select one of the insertion operators for the stations;
    Update I_o for the selected operator;
      Add the attributes of the applied operators to the tabu list;
    else if a route is removed **then**
      Select one of the insertion operators for customers;
      Update I_o for the selected operator;
      Add the attributes of the applied operators to the tabu list;
    else (if a customer is removed)
      Select one of the insertion operators for customers;
      Update I_o for the selected operator;
      Add the attributes of the applied operators to the tabu list;
    end if
    if the solution is not feasible **then**
      Apply Greedy Station Insertion operator;
    end if
    if $Cost(CurrentSolution) < Cost(BestSolution)$ **then**
      Update *Current Solution*;
      Update *Best Solution*;
      Update S_o s, W_o^i s, and $Probability_o^i$ s for operators;
      Remove the attributes of the applied operators from the tabu list;
    else
      if the attributes of the operators that have been used in *Current Solution* are not tabu **then**
        Update *Current Solution*;
        Update S_o s, W_o^i s, and $Probability_o^i$ s for operators;
        Update the tabu list;
      end if
    end if
  Until *IterIn* iterations have been done
Until *IterOut* iterations have been done
Output *Best;*

5.2. Multi-objective methods

Ropke and Pisinger (2006) and Demir et al. (2014) showed the effectiveness of multi-objective methods for solving the multi-objective pollution-routing problem. In this study, we use three different methods for solving the bi-objective model and for comparing the results: "weighted-sum", "ε-constraint", and "hybrid" methods.

A multi-objective problem is often solved by merging all the objectives into one single objective function. This technique is known as the weighted-sum method (Kim and De Weck, 2005; Marler and Arora, 2010; Wang et al., 2016). The formulation of the weighed-sum technique for our problem is shown in Eq. (30). ϖ_i is the associated weight of the objective function Z_i. The weights are nonnegative, and their summation should be one.

$$Min \varpi_1 Z_1 + \varpi_2 Z_2$$

$$\varpi_1 + \varpi_2 = 1 \tag{30}$$

Another popular solution technique for solving multi-objective optimization problems is the ε-constraint method (Mavrotas, 2009; Mavrotas and Florios, 2013; Yu and Solvang, 2016). In this technique, the decision-maker selects one of the objectives to be minimized, and the other objectives are transformed into constraints (Marler and Arora, 2004; Caramia and Dell'Olmo, 2020). In the mathematical model of this paper, Z_1 is considered the main objective function. In addition, Z_2 is written as one of the constraints. Therefore, the model is written as follows:

$$Min\, Z_1$$

$$Z_2 \le \varepsilon \tag{31}$$

The hybrid method is a combination of the weighted-sum and ε-constraint methods. In this technique, all objective functions are transformed into constraints. At the same time, the objective function is calculated as the weighted sum of all objective functions (Demir et al., 2014).

5.3. Multi-objective metaheuristic algorithm

We integrate the ALNS algorithm with multi-objective solution approaches described in the previous section. The ALNS algorithm without the SA or the TS approach has been combined with the multi-objective approaches since the ALNS algorithm shows a better performance based on the findings later presented in Section 6.4. After choosing and implementing the insertion and removal operators within the ALNS algorithm (See Algorithm 1), instead of only comparing the cost of the obtained solution with the cost of the best solution, the solutions are checked based on a modified objective function that is defined by one of the multi-objective solution approaches. If the current solution is better than the best solution found so far, the best solution is updated. In the weighted-sum approach, the objective function is set to the sum of weighted objectives instead of the cost of transportation. ϖ_i is set to 0 in the first iteration and then is increased by 0.1 after the specific number of algorithm iterations. The maximum value that ϖ_i can take equals 1 (See Eq. (30)). The solutions for ϖ_i ($i = 1, \cdots, 11$) are saved and compared with each other. Then, the solutions not dominated by any other solutions are kept as Pareto solutions. Since enough Pareto solutions have been produced for this problem, we did not increase the number of weights to generate more solutions.

For the ε-constraint method, first the ALNS algorithm is implemented to find the best solution for minimizing the second objective which is fuel consumption. The algorithm is rerun to find the minimum value for the first objective function (the cost of transportation), while the second objective (fuel consumption) has to be equal to or less than its minimum value. Then, after a fixed number of iterations, this minimum value which is the amount of consumption was increased by ε. The procedure is repeated 11 times to run the model an equal number of times compared to the weighted-sum method. It should be noted that the value of ε is determined after a primary parameter tuning. Finally, the Pareto solutions are obtained by finding the non-dominated solutions among the 11 generated solutions.

For the hybrid approach which is the combination of ε-constraint and weighted-sum methods, the algorithm is run to obtain the best value for fuel consumption. This step is similar to the ε-constraint method, and the fuel consumption is set to be equal to or less than the best value. After a certain number of iterations, the amount of the best value is increased by ε. However, instead of running the algorithm for finding the best value for the first objective function, the minimum value of the weighted sum of both objectives is calculated. This process is also repeated 11 times and Pareto solutions are determined from all the obtained solutions.

6. Computational studies

To evaluate the proposed solution approaches, an application with real-world locations in parts of Ontario, Canada is described in Section 6.1. In addition, the real-world parameters related to the heavy-duty electric trucks that are currently sold in the North American market are introduced. The results of applying the solution methods are given in Section 6.2, Section 6.3, Section 6.4., and Section 6.5. The related numerical analysis for single objective and bi-objective models are also presented in these subsections. The data and codes are publicly available via GitHub.[2]

6.1. Experimental design

Walmart in Canada aims to convert its fleet to electric vehicles by 2022 and entirely alternative fuel vehicles by 2028. The company has ordered 130 Tesla semi-trucks (Electric Autonomy, 2020), with the first 20 trucks will be used in the Mississauga distribution location (Green Car Congress, 2018). The Tesla semis are considered class 8 heavy-duty trucks with 36-tonne payloads. According to Walmart Canada (2021), each distribution center covers nearly 135 stores on average in a 500-kilometer weighted average distance. This means that the trucks visit supercentres at shorter distances in high-density areas such as the Greater Toronto Area (GTA). In addition, based on Walmart Canada Corp. (2021) news, a new distribution center has been opened in Cornwall, Ontario, to cover 136 supercenters from Kingston, Ontario, to Canada's east coast.

Furthermore, another distribution center will be constructed in Moncton, New Brunswick, to cover 43 stores (Supermarket News, 2021). According to the reports mentioned above, Walmart Canada intends to reduce long-haul distances to provide a more sustainable and reliable supply chain. Hence, a subset of stores within 100 km of the Mississauga distribution location has been selected to solve the problem for shorter distances.

Currently, Walmart Canada owns a fleet of 180 tractors and 2,000 trailers. These statistics reveal that Walmart requires a routing plan that considers both electric and diesel trucks at the same time. This situation is somewhat similar for other logistic companies that intend to electrify their fleets such as UPS and Amazon. To provide insights for logistics companies that are going to use heavy-duty electric trucks for short-haul distances, we investigate the problem using the example of Walmart since there is enough evidence that Walmart is going to add heavy-duty electric vehicles to its fleet for distribution in the denser areas. Hence, a distribution center and the supercenters within 100 km of it are chosen to address the routing of heavy-duty trucks for shorter distances. Although we intend to use accurate and real-world data, because heavy-duty electric trucks are not yet deployed widely, some of the parameters, such as the locations of stations, are hypothetically considered based on the existing data. For this reason, the problem of routing a mixed-fleet of vehicles for a Walmart distribution center as the depot and its supercenters as customers is solved in this paper, considering the specifications of electric heavy-duty trucks.

Based on the reviewed literature and practical reports, the potential influence of three factors including the service area, the density of charging stations, and recharging power are investigated for this problem. These factors are the main features that need to be studied for utilizing electric heavy-duty trucks in short-haul delivery. First, due to the limited travel range of heavy-duty trucks, the area of the service can be essential for routing these vehicles. The second concern is related to the number of charging station infrastructures throughout the service area. Finally, the charging technology is another obstacle in using heavy-duty trucks since the vehicles need to receive a considerable amount of charge in a reasonable time. All these factors are investigated at two levels.

Service area: Walmart supercenter locations in the GTA are considered as the customers in a small service area, whereas the supercenters within 100 km of GTA are accounted as the customers in a large service area. We have chosen these 80 supercenters located in southern Ontario due to the higher population density in this area. Therefore, the number of supercenters in the small and large areas equals 20 and 80, respectively.

Station density: Since stations with charging power that is suitable for recharging heavy-duty electric trucks are very rare throughout Ontario, we consider some potential locations for the charging stations. These locations are selected to ensure that the distance between each pair of stations is less than 50 km to guarantee enough charge for traveling between the charging stations. When the number of stations is low, the density is identified as low, and when this number is doubled, the density of stations is called high. The numbers of charging stations are set to 4 (low), and 8 (high) in the small service area. In addition, they are considered 16 (low) and 32 (high) for the large service area. Fig. 1

[2] https://github.com/afsane-amiri/A-Bi-objective-GVRP-with-a-Mixed-fleet-Codes-Data.git.

and Fig. 2 depict the depot, supercenters, and stations' locations. The real locations of Walmart supercenters in Ontario have all been extracted from Walmart's store locator on their website (Walmart, 2021). The yellow house denotes the depot, which is the Walmart Canada Logistics in Mississauga, in Fig. 1 and Fig. 2. Based on Walmart website, 80 supercenters are located within 100 km of the Mississauga distribution center. The red pins represent the real locations of supercenters in southern Ontario and the GTA (Walmart, 2021).

According to Electrify Canada (2021), there are a few charging stations with powers of 90 and 350 kW in the examined area. The locations of these stations are assumed to be as some of the charging stations. Based on reports (e.g., Government of Canada, 2021c; Truck News, 2021), suitable stations for heavy-duty trucks will be built as part of the effort to utilize heavy-duty electric trucks. Moreover, NACFE evaluates the regions in Canada and the US by considering factors including charging infrastructure, funding, incentives, and the need to reduce GHG emissions. NACFE indicates that the GTA is among the high-potential regions for deploying heavy-duty electric trucks in short-haul operations (Electric Truck Guidance Report Series, 2020). Furthermore, more than 250 public charging stations with DC fast chargers are available for passenger cars in Ontario (Plug'n Drive, 2021). Similar to the passenger cars, the heavy-duty charging stations' infrastructures will be provided on a large scale once the heavy-duty trucks are produced en masse.

Based on the above-mentioned reports, the rest of the charging stations were added to Fig. 1 and Fig. 2 to consider the future progress in the availability of stations. Finally, the blue stations represent their locations in the low-density case, and the green ones represent the added stations for the high-density case.

Charging power: Charging at the depot and charging with fast chargers throughout the route are considered as the charging options for heavy-duty electric trucks. According to Electrify Canada (2021), two charging options are available with powers of 90 kW (low) and 350 kW (high). The costs are 0.27 per minute for the low power, and 0.57 per minute for the high power. Considering these three factors at two levels results in 8 combinations. After some initial evaluations, 7 instances for each combination are taken to eliminate the random effect. Then, to ensure independence within the combinations, the locations of the supercenters are randomly selected for each instance. In total, 8 combinations with 56 instances are created.

The other related parameters are generated based on the latest literature and reports about the current available heavy-duty trucks. Existing electric trucks equipped with a 350-kWh battery can cover 200 km in a range which are provided by BYD company (Liimatainen et al., 2019). The purchasing cost for this model is \$150,000 (TESMANIAN, 2020), whereas the average price for the same diesel truck is around \$125,000. Energy consumption for the electric vehicle is 1.75 kWh/km, while the number is 2.5 times larger for the diesel vehicle. Based on a report by Trucks.com (2019), the operating cost for electric trucks is almost \$2.75, while this number is \$3.30 for a comparable diesel truck.

The payload for BYD trucks is almost the same as for diesel trucks and equals 36 tonnes (Liimatainen, et al., 2019). The demand for each supercenter is generated by choosing a random number between 10 and 50 percent of the payload. Based on several reports (Talk Business & Politics, 2018; Puls News, 2022; MBA Knowledge Base, 2022), it takes 2 hours to unload a 36-tonne trailer at Walmart supercenters. Considering the set-up time for unloading the trailer and other possible delays in the process of unloading, the time required for unloading every tonne of the load is assumed to be between 3 and 5 min. Therefore, the service time for each demand is obtained by multiplying the demand and a random integer between 3 and 5. Given that the driving shift generally takes 8 hours a day, Given that the driving shift takes typically 8 h a day, 2-hour and 4-hour time windows are randomly generated during 8-hour shifts, inspired by practical cases such as Walmart's distribution system (MBA Knowledge Base, 2022). For calculating the labor cost, the median for a heavy-duty truck driver's salary in Canada is about \$23 per hour (Nauvoo, 2020).

The front area of heavy-duty trucks is 7.2 m^2 (Sripad and Viswanathan, 2017). We use average numbers for the acceleration rate and road angles which are equal to 0.68 ($\frac{m}{s^2}$) (Yang et al., 2016) and 4.57 degrees,

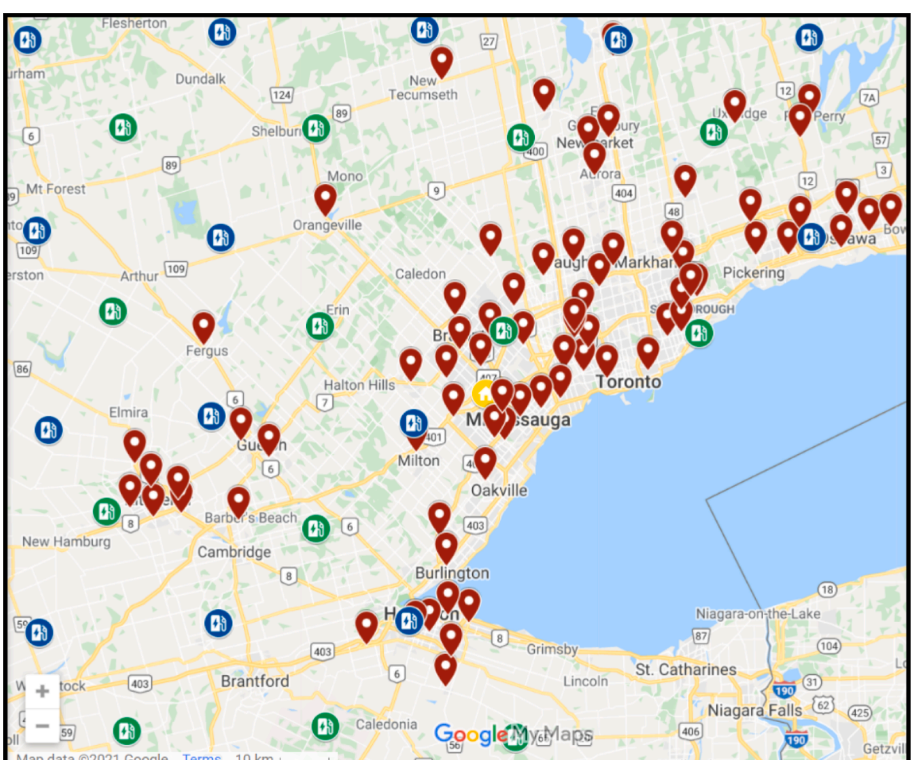

Fig. 1. Distribution of locations in the large service area.

Fig. 2. Distribution of locations in the small service area.

respectively. The road angle is obtained by calculating the inverse tangent of the superelevation rate. The acceptable superelevation rate is 0.06 (Transportation Association of Canada, 2017). The values of the parameters are shown in Table 3.

6.2. CPLEX results

The results of implementing CPLEX on the single objective and bi-objective mathematical models for small-size instances are presented in Table 4. The results are compared to those obtained by applying the developed metaheuristic algorithm to the same instances. The total number of vertices for small-size instances has been determined after running several instances with different numbers of vertices. Finally, CPLEX could optimize the instances with 13 vertices or fewer. Therefore, we solved the mathematical model for five different instances with ten customers, two stations, and a depot with a time limit of three hours. With the small number of customers and shorter distances, where there is no need for recharging, EVs are more likely to be used. In this case, the second objective function can not be analyzed for small instances when all the vehicles are electric. Therefore, the number of available EVs is restricted in small instances to observe the performance of the model in the presence of both types of vehicles. The rest of the parameters were considered similar to those defined in the previous subsection. Since small-size instances can be solved to optimality using the CPLEX solver, we can use the obtained solutions from CPLEX to evaluate the performance of the developed ALNS algorithm. As such, these test instances are solved by using CPLEX solver and the ALNS algorithm. The "Objective Function Value" column of Table 4 depicts the results of solving the single-objective problem by CPLEX solver to optimality. For all these small instances, the ALNS method could obtain the optimal solutions in a much shorter time. For evaluating the bi-objective model, a weighted-sum method with $\varpi_1 = 0.5$ has been chosen to merge the objectives. The results of solving the bi-objective problem for both the CPLEX and the ALNS algorithm are shown in the column labeled "Bi-objective Function Value". A similar observation can also be made for the case of the bi-objective problem when both objectives are given the same weight. Since we want to investigate the impact of the main factors of EVRP and the trade-offs between two objectives in a real-world situation with a realistic number of vertices, we do not present the

Table 3
The parameters' values used in experiments.

Parameter	Average value
Battery capacity	350 kWh
Purchasing Cost for EVs	\$150,000
Purchasing Cost for CVs	\$120,000
Energy Consumption for EVs	1.75 kWh/km
Energy Consumption for CVs	4.375 kWh/km
Operating Cost per kilometer for EVs	\$2.75
Operating Cost per kilometer for CVs	\$3.30
Labor cost per hour	\$23
Total weight of the vehicle W_T	37,000 kg
Gravitational acceleration G	9.81 m/s^2
Rolling resistance coefficient C_r	0.01
Aerodynamic drag coefficient C_a	0.7
Air density φ	1.2041 kg/m^3
The frontal area of the vehicle A_v	7.2 m^2
fuel-to-air mass ξ	1
Acceleration τ	0.68 m/s^2
The angle of the road	4.57°

Table 4
Results for small-size instances.

Instance	Single Objective Function Value (\$)	CPLEX Time (*sec*)	ALNS Time (*sec*)	Bi-objective Function Value	CPLEX Time (*sec*)	ALNS Time (*sec*)
1	1,753.78	34.70	3.80	877.31	68.63	5.87
2	1,667.26	87.41	3.41	833.94	84.33	5.30
3	1,676.75	54.57	3.50	838.71	66.60	5.06
4	1,697.54	25.67	3.74	849.14	22.77	6.03
5	1,705.82	46.84	3.68	853.29	38.93	5.67
Average	1,700.23	49.84	3.63	850.48	56.25	5.59

numerical analysis on the small-size instances. To avoid redundancy, all the numerical analysis of the problem is just shown for the designed instances in the next sections.

6.3. Results for EVRPTW benchmark instances

To investigate the efficiency of the presented ALNS algorithm, we compared its performance against the solutions for the EVRPTW instances in Keskin and Çatay (2016). Keskin and Çatay (2016) proposed a solution method for EVRPTW with partial recharge but also solved problems with full recharge to validate their algorithm with solutions reported by Goeke and Schneider (2015) and Hiermann et al. (2016). To solve the benchmark instances, we modified our model by removing the second objective, replacing all the cost components of the first objective with the total traveling distance, and considering full recharge. Since the customers in our generated instances are located in a clustered manner (i.e., concentrated in metropolitan areas, as seen in Fig. 1), we evaluate the performance of our proposed algorithm against clustered sets of the EVRPTW instances. The obtained results are reported in Table 5. Even though our proposed algorithm is designed for a different problem with mixed-fleet, partial recharge, and different cost components, the average gap (expressed in percentages) from the solutions in Keskin and Çatay (2016) is negligible. Also, our developed approach outperforms in 9 out of 17 benchmark instances. The average gap of below 1 % and the number of improvements (9 out of 17) indicate that the proposed algorithm performs well even for large instances.

6.4. Single objective model results analyses

The solution approaches are programmed in visual C++ and run on a Core i5 3.40 GHz computer with 8 GB of RAM. ALNS methods have been implemented for the mathematical model with the single objective of minimizing the total cost to determine the impact of the three main factors we have mentioned in the previous subsection. Table 6 provides the objective values and running times for all 56 instances. The second column represents the characteristics of the test instances according to the service area (S stands for small whereas L stands for large), the station density (L for low and H for high), and the charging power (L for low and H for high).

The results of solving the problem by applying ALNS combined with the TS diversification approach are shown in the columns labeled "ALNS-TS". While the results of using ALNS with the SA approach are shown in columns labeled "ALNS-SA". The last columns identified by

Table 5
Comparison with the solutions of EVRPTW instances.

	Our proposed ALNS		Keskin and Çatay (2016)		Deviation	
Instance	Total Distance	# of EVs	Total Distance	# of EVs	Gap	Gap Percentage
c101	1,072.43	12	1,053.83	12	0.02	1.76
c102	1,090.90	12	1,056.12	11	0.03	3.29
c103	1,037.98	11	1,034.86	11	0.00	0.30
c104	1,044.49	10	951.57	10	0.10	9.76
c105	**1,068.62**	12	1,075.37	11	**−0.01**	**−0.63**
c106	**1,042.17**	11	1,057.65	11	**−0.01**	**−1.46**
c107	1,046.19	11	1,031.56	11	0.01	1.42
c108	**1,069.31**	12	1,095.66	11	**−0.02**	**−2.41**
c109	1,092.81	12	1,033.67	10	0.06	5.72
c201	**629.95**	4	645.16	4	**−0.02**	**−2.36**
c202	**629.95**	4	645.16	4	**−0.02**	**−2.36**
c203	**629.95**	4	644.98	4	**−0.02**	**−2.33**
c204	639.93	4	636.43	4	0.01	0.55
c205	**629.95**	4	641.13	4	**−0.02**	**−1.74**
c206	**629.95**	4	638.17	4	**−0.01**	**−1.29**
c207	643.07	4	638.17	4	0.01	0.77
c208	**630.86**	4	638.17	4	**−0.01**	**−1.15**
Average	**860.50**	**7.94**	**853.98**	**7.65**	**0.00**	**0.46**

"ALNS" are the results of applying the ALNS algorithm without any diversification approaches. By comparing the results of the algorithms, it can be observed that the ALNS algorithm, without any diversification approaches, has a slightly better performance in terms of the average of the objective values and CPU time. Unlike some studies in the literature (Goeke and Schneider, 2015; Keskin and Çatay, 2016; Koç et al., 2019) that reported high-quality results by using ALNS-SA, the obtained results from the ALNS demonstrate a high solution quality when appropriate operators are selected, and the parameters are set carefully. The quality of ALNS will be evaluated in more detail in the following section.

It is evident that by increasing the number of customers from 20 to 80, the averages run times for the algorithms rise. The average values of the running times indicate that even for a large service area, the proposed algorithms can obtain the solutions in less than 5 min, which is a reasonable time for solving routing problems.

After solving the instances, a regression model is applied for the ALNS results, which have a better performance to statistically analyze (e.g., Zolfagharinia & Haughton, 2017, 2018) the impact of the three main factors on the cost. Table 7 includes the details of the statistical analysis. The interaction of all three factors and pairwise interactions are investigated in the regression model. The *P*-values indicate that all three factors have a statistically significant effect on the cost. First, it is evident that the service area is effective on the cost because traveling in larger areas results in higher costs for the company. Secondly, increasing the number of charging stations allows companies to utilize more EVs and reduce transportation costs. Therefore, this factor influences the value of the objective function. Thirdly, improving the charging power enables the drivers to charge their EVs faster and reduce costs.

Among the interactions provided in Table 6, there are considerable mutual interactions between the station density and service area, as well as the charging power and the station density. Fig. 3 clarifies this relation by comparing the values of objectives at each level of these two factors. When the density station is (specified by blue bars), enhancing charging power yields a 5.5 % reduction in the total costs from 13,473.66 to 12,711.58. In the higher density (red bars), there is a 5 % percent reduction in the total costs by increasing the charging power. In addition, with low charging power, the total cost will decrease by 2 % if the number of stations is increased. Lastly, there is a slight decrease in the total cost where the charging power is high and the station density is changed from low to high. These findings reveal that it might be more economical in the current situation to focus on only improving one of these two factors.

Table 8 shows the average results for each cost component in small and large service areas. As seen from this table, in the small service area where the number of EVs used is greater than the number of CVs, the acquisition costs cover a larger portion of the total costs than the other two cost components. At the same time, the traveling costs are the biggest cost component for the large service area where more CVs are used to visit the customers. The last column also reveals that the charges are rarely used in small service areas, whereas, in the large service area, approximately eight chargers have been used on average for each instance. In addition, the overall traveling distance of EVs is larger than CVs in small areas because EVs are more attractive (i.e., charging is less required for shorter distances). The reverse is true in larger areas since CVs can be used without driving range concerns.

6.5. Bi-objective model results analyses

The bi-objective model is solved to gain insights into the emissions and the trade-offs between the two objective values. The computational results for the bi-objective model for the instances are provided in Table 9. The first set is characterized by the small service area, low station density, and low charging power. The station density is considered high in the second set, while the charging power is high in the third one. The fourth set has high charging power and high station density in the small service area. In the fifth set of instances, low charging power

Table 6
The results for the single objective model.

Algorithm		ALNS-SA		ALNS-TS		ALNS	
# of instance	Combination	Obj. ($)	Time (*Sec.*)	Obj. ($)	Time (*Sec.*)	Obj. ($)	Time (*Sec.*)
1	SLL	3,477.54	12.36	3,495.29	6.28	**3,427.70**	**4.83**
2		**3,321.80**	13.23	3,338.96	**1.85**	3,325.65	**1.78**
3		**3,263.44**	11.49	3,288.91	**6.13**	3,301.71	6.36
4		**3,285.91**	11.90	3,288.28	**1.51**	3,307.19	1.85
5		3,335.78	11.59	3,380.44	**4.05**	**3,278.28**	4.37
6		3,331.74	**4.36**	**3,324.70**	6.20	3,366.20	6.18
7		3,327.53	11.67	3,316.99	**3.50**	**3,323.14**	3.53
8	SHL	**3,309.89**	11.73	3,346.52	5.02	3,314.29	**4.71**
9		**3,332.78**	13.91	3,344.59	2.14	3,351.73	**1.74**
10		3,307.96	12.60	**3,299.78**	5.36	3,331.94	**4.24**
11		3,300.03	12.04	3,244.25	**1.87**	**3,228.35**	1.98
12		3,305.89	11.89	3,323.60	4.43	**3,294.84**	**4.04**
13		3,213.14	10.80	**3,202.80**	**4.14**	3,231.57	5.09
14		3,358.07	11.56	3,391.70	**2.06**	**3,345.54**	3.89
15	SLH	**3,202.93**	10.98	3,272.71	**3.68**	3,212.11	4.12
16		**3,298.36**	11.80	3,353.29	**1.56**	3,299.45	1.67
17		**3,264.23**	11.67	3,299.17	**3.33**	3,275.52	5.10
18		3,321.09	11.97	**3,289.81**	**4.35**	3,297.54	4.97
19		3,321.09	12.05	**3,289.81**	**4.21**	3,297.54	4.97
20		**3,258.92**	11.69	3,311.22	4.61	3,293.14	**4.24**
21		**3,288.26**	11.60	3,289.62	3.71	3,293.71	3.01
22	SHH	**3,259.54**	12.23	3,280.56	**4.40**	3,315.03	5.40
23		3,360.65	12.43	**3,332.67**	2.30	3,378.97	**1.73**
24		**3,278.96**	11.52	3,298.31	4.47	3,289.31	**4.32**
25		**3,304.95**	12.68	3,349.05	**0.95**	3,299.93	1.41
26		**3,263.64**	11.88	3,274.29	7.10	3,274.59	**7.07**
27		**3,344.75**	11.23	3,346.94	**5.51**	3,372.98	5.98
28		**3,384.83**	11.28	3,389.19	**3.57**	3,410.29	3.58
29	LLL	**22,423.59**	193.01	22,578.92	166.34	22,532.44	**134.32**
30		**23,932.49**	218.77	24,073.98	**151.66**	24,073.98	167.19
31		25,062.65	208.10	24,556.19	205.11	**23,614.22**	**167.42**
32		24,961.44	205.31	24,209.32	182.14	24,515.08	**177.02**
33		**22,935.57**	209.31	24,496.37	**156.24**	24,066.39	166.06
34		24,505.81	204.33	24,505.81	177.56	**22,969.09**	**176.84**
35		24,248.67	209.97	**23,349.21**	207.02	23,530.11	**170.69**
36	LHL	23,884.74	296.04	**23,263.02**	276.57	22,296.86	**258.72**
37		**24,221.03**	360.09	24,653.55	**268.92**	24,653.55	288.06
38		22,352.51	371.17	22,536.70	337.34	**22,105.98**	**279.08**
39		23,087.36	339.03	**22,402.30**	320.95	23,010.04	**315.80**
40		23,811.93	344.99	23,386.91	330.92	**21,840.01**	**325.62**
41		24,638.29	377.15	26,137.61	384.15	**23,608.65**	**311.66**
42		**23,562.24**	365.36	23,768.14	294.48	24,123.21	296.70
43	LLH	22,174.01	138.58	21,386.53	**81.07**	**21,008.74**	92.42
44		23,257.30	143.23	22,215.43	114.10	**21,994.36**	**107.82**
45		**22,732.92**	146.68	22,819.66	124.38	22,925.92	**121.64**
46		23,039.15	137.22	23,423.34	117.87	**21,935.15**	**106.60**
47		22,835.26	133.22	**22,479.36**	98.52	23,096.88	**97.69**
48		**21,974.36**	126.90	22,470.05	**84.64**	22,040.68	107.90
49		22,647.74	154.05	**21,991.33**	125.72	**21,991.33**	**120.98**
50	LHH	22,177.27	170.86	**20,965.54**	138.75	21,904.95	**113.90**
51		22,769.98	215.80	22,717.86	202.27	**22,184.26**	**163.17**
52		22,817.30	202.55	22,254.87	187.42	**21,481.33**	**174.79**
53		21,952.85	189.76	22,581.59	**175.90**	**21,916.93**	178.85
54		23,186.05	204.62	22,878.63	**149.92**	**21,945.03**	158.88
55		22,125.70	203.20	21,936.23	**164.01**	**21,829.43**	170.93
56		**21,806.10**	222.43	22,953.04	209.20	22,822.82	**144.71**
Average		13,245.50	118.18	13,213.48	98.95	**13,013.49**	**92.99**

NOTE. SLL = Small service area, Low density, Low power; SHL = Small service area, High density, Low power; SLH = Small service area, Low density, High power; SHH = Small service area, High density, High power; LLL = Large service area, Low density, Low power; LHL = Large service area, High density, Low power; LLH = Large service area, Low density, High power; LHH = Large service area, High density, High power.

and low station density are considered in the large service area. The station density is high in the large service area for the sixth set. However, the charging power is low. In the seventh set, the station density is low while the charging power is high. Finally, both factors are considered high in the last set. The average running times for each method to solve all eight sets, including seven instances, are reported in Table 9. As seen, the methods perform efficiently in terms of computational time. Instances are solved within 251.5, 279.7, and 243.8 s on average by the weighted-sum, ε-constraint, and hybrid methods, respectively. This time is reported based on 25,000 iterations. The average computational time for small area instances is 15.5 s, and for the large area is 487.5 s in the weighted-sum method. These numbers are 15.4 and 544 s for the ε-constraint method. The hybrid method requires almost the same computational effort as the weighted-sum method. Regarding the quality of multi-objective solution methods, three values are calculated for the presented methods. The number of Pareto solutions, the values of the ε-indicator, and the hypervolume indicator are shown in Table 9. Regarding the number of Pareto solutions, the weighted-sum method performs better than the other with 2.6 Pareto solutions. Evaluating the performance of the solution methods in multi-objective programming

Table 7
Coefficient tests and *P*-values for the regression model for the average costs.

	Coefficients	*t* stat	*P*-value
Intercept	9,970.32	218.49	**1.28E-73**
Service Area	−127.57	163.15	**1.54E-67**
Station Density	−312.05	−2.09	**0.042186**
Charging Power	−136.65	−5.11	**5.61E-06**
Service Area*Station Density	−314.80	−2.24	**0.030037**
Service Area*Charging Power	−29.78	−5.15	**4.81E-06**
Station Density*Charging Power	9,970.32	−0.49	0.628309

NOTE. * denotes the interactions.

models is different from single-objective optimization models. While the results of single-objective models can be compared with the optimal solutions produced by exact methods, the results of multi-objective methods are a set of Pareto solutions. The most prevalent way of assessing multi-objective solution approaches is the number of Pareto solutions (Demir et al., 2014). We use two quality assessment techniques to compare the presented methods. These techniques, called hypervolume and ε-indicators, have been introduced by Zitzler and Thiele (1998) and Zitzler et al. (2003).

The hypervolume technique in two dimensions calculates the area of the rectangles which can be drawn between each pair (Z_1, Z_2) in the obtained solution set of the method and the reference point (Zitzler and Thiele, 1998). The reference point in this study is the worst (maximum) value obtained by that method for each objective function. The union of all the rectangles is the value of the hypervolume indicator. The method with the larger value of the indicator is considered the better solution method.

The ε-indicator is performed based on multiplicative ε-dominance relation (Zitzler et al., 2003). In the bi-objective optimization, the best values of the first and the second objectives from all known Pareto solutions (Z_1^*, Z_2^*) are obtained. If the minimum values for Z_1 and Z_2 that are found by Method i are indicated as (Z_1^i, Z_2^i), then the differences between Z_1^* and Z_1^i, and Z_2^* and Z_2^i are calculated for Method i as (Δ_1^i, Δ_2^i). The maximum value of Δ_1^i and Δ_2^i is kept as the ε-indicator value for the i^{th} method. The method with the lowest value of the indicator is the method with the best performance.

By calculating the indicators, we can observe that the weighted-sum method performs remarkably better than the ε-constraint and hybrid methods. The weighted-sum method has the minimum value for the ε-indicator, and the maximum value for the hypervolume indicator. ε-constraint and hybrid methods have almost the same performance, which indicates that the ε-constraint method does not work efficiently in this problem. These results reveal that the weighted-sum method is better suited to this problem.

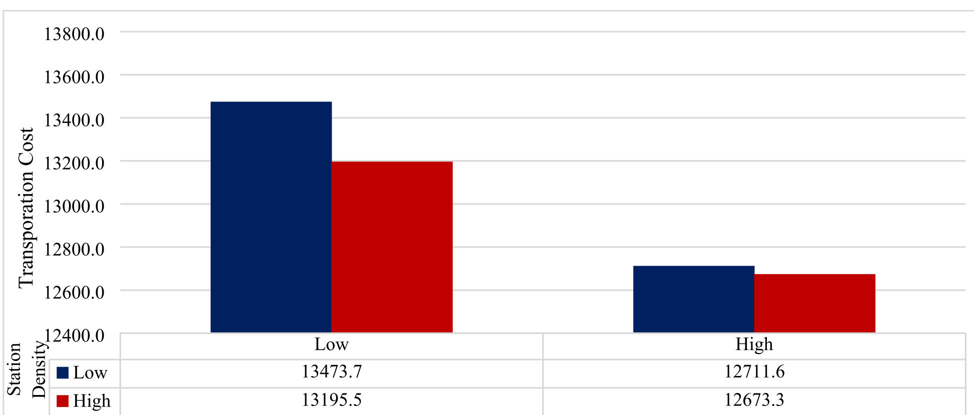

Fig. 3. Interaction of charging power and station density.

Table 8
Detailed results based on service area.

Area	Total Costs ($)	Acquisition Costs ($)	Charging Costs ($)	Traveling Costs ($)	Distance traveled by EV (km)	Distance traveled by CV (km)	# of EV	# of CV	# of Recharges
S	3,312.1	1,701.4	12.8	1,597.1	496.9	68.6	5.0	1.0	0.5
L	22,714.9	7,465.4	43.9	15,168.6	2,120.9	2,830.7	12.2	14.6	7.8

Table 9
Results of the bi-objective methods.

Method	Weighted-sum				ε-constraint				Hybrid			
Set	Avg. # of Pareto solutions	Hypervolume indicator (I_{hv})	ε-indicator (I_ε)	Time	Avg. # of Pareto solutions	Hypervolume indicator (I_{hv})	ε-indicator (I_ε)	Time	Avg. # of Pareto solutions	Hypervolume indicator (I_{hv})	ε-indicator (I_ε)	Time
1	2.7	1,578,007.1	28.9	15.7	1.9	109,748.1	4.7	15.8	1.4	1,593,784.9	12.9	15.1
2	2.9	1,316,320.3	21.4	15.7	1.7	122,776.3	33.1	15.5	2.0	1,366,296.4	8.1	15.3
3	2.7	1,242,296.0	14.6	14.7	2.4	76,323.0	29.4	15.3	1.4	1,257,602.2	5.2	14.5
4	2.4	1,643,661.3	19.4	16.0	1.3	97,688.1	14.0	15.0	2.3	1,630,849.4	13.3	15.5
5	2.3	1,605,043.2	268.7	446.6	1.3	4,171,686.3	1,568.2	593.3	1.4	1,335,044.8	1,369.1	454.9
6	2.4	2,921,512.6	10.6	816.1	1.3	10,061,340.4	1,119.2	780.2	1.4	2,933,558.0	1,085.2	724.0
7	2.9	13,260,231.1	104.4	259.6	2.1	2,931,677.9	389.0	327.3	2.1	12,898,518.5	242.6	296.0
8	2.6	9,712,579.8	395.3	427.6	2.1	3,108,840.9	659.1	475.3	2.0	7,068,457.8	473.3	415.2
Average	**2.6**	**4,159,956.4**	**107.9**	251.5	1.8	2,585,010.1	477.1	279.7	1.8	3,760,514.0	401.2	243.8

Table 10
Extreme and average of Pareto solutions from Set 5 to Set 8 with the weighted-sum method.

Set	Transportation costs ($)			Fuel consumption (Liter)		
	Min.	Max.	Avg.	Min.	Max.	Avg.
5	21,924.8	25,761.4	24,298.8	810.9	1,309.0	1,022.9
6	21,725.7	26,012.4	23,964.4	662.8	1,091.7	938.8
7	21,372.6	24,108.7	22,764.8	342.2	1,161.4	705.1
8	21,482.7	23,643.5	22,618.1	186.2	946.8	651.1

The results for the instances of Set 5 to Set 8 are discussed to study the impact of station density and charging power in the large service area. We do not discuss the case of the small service area because it is less likely for EVs to visit the charging stations in the small area. Also, it is less likely to use CVs, and the second objective value could be negligible. For the trade-off analysis, the results of the weighted-sum method are considered due to better performance. The detailed results, such as the minimum, maximum, and average values of costs and fuel consumption for Sets 5–8, are shown in Table 10.

As shown in Table 10, the best value for the average transportation costs is obtained by instance Set 8 for $22,618.1. This is because set 8 represents a situation where the charging power and the density of stations are high. Furthermore, as shown in Table 10, Set 8 also has the lowest average fuel consumption with 651.1 Liters. It can thus be revealed that by increasing the number of stations and improving the technology of chargers, delivery companies can experience a reduction in their transportation costs and GHG emissions.

The lower values of the average costs for instances of Set 6 in comparison with those of Set 5 occur because as the number of stations rises, the number of utilized EVs also increases. Therefore, the costs are decreased. Furthermore, the lower average values of the costs and fuel consumption for the results of instances of Set 7 compared to the results of instances of Set 5 indicate that by increasing the speed of charging, the delivery companies can have fewer costs and produce lesser amounts of GHG emissions.

After discussing each set's average costs and fuel consumption, the trade-off curves between these two objectives are investigated. First, the trade-off graph is plotted for one instance as an example of Set 6 where the density of stations is high, and the charging power is low. The values on the vertical axis show transportation costs (Z_1), while the values on the horizontal axis present fuel consumption (Z_2). Fig. 4(a) discloses that by increasing 10 % of the transportation costs, delivery companies can reduce more than 15 % of fuel consumption. In addition, Fig. 4(b) illustrates the same behavior for an instance of Set 7. Based on this figure, by increasing 7 % of the cost, fuel consumption can be reduced by 34 %. The detailed results of the trade-off between all the instances for each set are shown in Tables 11 and 12. In these tables, the values for the lowest costs and the second-lowest costs are presented with their corresponding fuel consumption values. The average percentages of the differences reveal that by increasing a small amount of cost (almost 2 %), delivery companies can create a remarkable reduction in fuel consumption (by more than 18 %), which leads to decreased GHG emissions.

7. Conclusions

This paper presented a new green vehicle routing problem, including electric and conventional heavy-duty trucks. Furthermore, it proposed a bi-objective mathematical model in which the first objective is the minimization of transportation costs, while the second one is the minimization of GHG emissions. First, we developed the ALNS algorithm for solving the model with the first objective. Then, we integrated three multi-objective solution techniques, including the weighted-sum, ε-constraint, and hybrid methods, with the ALNS algorithm to generate the Pareto solutions for the bi-objective model. To the best of our knowledge, there has not yet been a study that developed a bi-objective model for the vehicle routing problem with a mixed-fleet of electric and conventional vehicles. Furthermore, previous studies focused more on the solution approaches of the EVRPs rather than their application in real-world settings. In contrast, we focused on several main factors in the EVRPs, comprising the service area, charging power, and density of

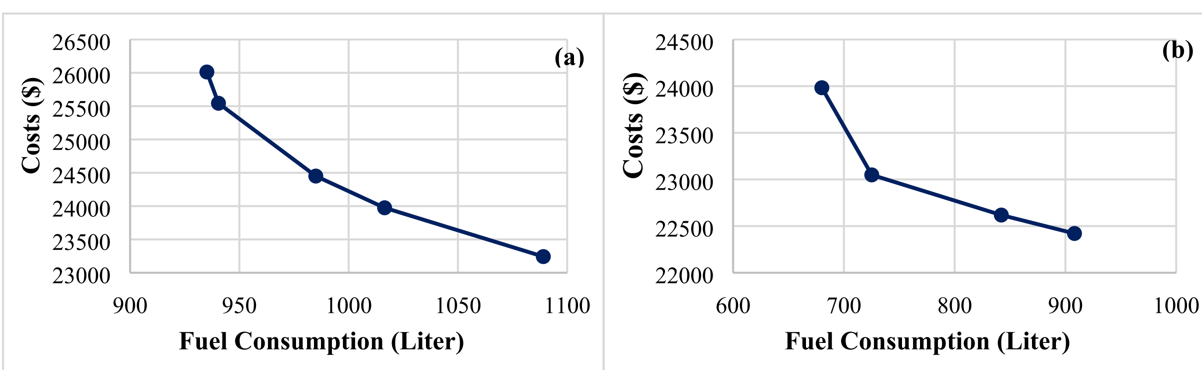

Fig. 4. Pareto solutions found for one of the instances for Sets 6 and 7.

Table 11
Trade-off analysis for Set 6.

Instance	Min. cost ($)	Corresponding Consumption (Liter)	Second lowest cost ($)	Corresponding Consumption (Liter)	Cost increase ($)	% of increase	Consumption reduction (Liter)	% of reduction
1	22,805.8	1,203.2	22,984.7	787.1	178.95 ↑	0.8	−416.08 ↓	−34.6
2	22,414.2	1,245.5	23,786.7	1,084.6	1,372.55↑	6.1	−160.86↓	−12.9
3	23,375.3	1,091.7	23,498.0	662.8	122.71↑	0.5	−428.91↓	−39.3
4	23,242.5	1,089.1	23,974.9	985.0	732.38↑	3.2	−104.12↓	−9.6
5	23,168.5	1,154.0	23,952.8	851.4	784.21↑	3.4	−302.57↓	−26.2
6	25,434.0	1,389.2	25,768.1	1,045.9	334.12↑	1.3	−343.28↓	−24.7
7	22,786.7	1,217.5	23,068.5	1,002.1	281.82↑	1.2	−215.42↓	−17.7
Average					587.5	**2.6**	−292.6	**−24.6**

Table 12
Trade-off analysis for Set 7.

Instance	Min. cost ($)	Corresponding Consumption (Liter)	Second lowest cost ($)	Corresponding Consumption (Liter)	Cost increase ($)	% of increase	Consumption reduction (Liter)	% of reduction
1	21,372.6	564.6	22,228.1	495.9	855.41↑	4.0	−68.69↓	−12.2
2	22,421.1	908.2	22,618.3	842.1	197.26↑	0.9	−66.05↓	−7.3
3	22,546.3	1,161.4	23,413.0	901.4	866.69↑	3.8	−259.98↓	−22.4
4	22,173.7	1,158.0	22,768.8	863.0	595.11↑	2.7	−295.02↓	−25.5
5	22,814.6	823.0	22,816.5	601.4	1.82↑	0.0	−221.58↓	−26.9
6	22,071.3	760.9	22,485.4	625.7	414.14↑	1.9	−135.18↓	−17.8
7	22,567.9	1,032.0	23,075.1	608.0	507.23↑	2.3	−424.04↓	−41.1
Average					488.4	**2.2**	−174.4	**−18.7**

recharging stations.

The results of the single objective version of the problem (i.e., the minimization of the transportation costs) have shown that the density of the stations and the charging power are influential factors in the transportation costs of the short-haul delivery problem with heavy-duty trucks. However, it has been observed that most of the benefit is achieved by either improving the charging power or increasing the density of charging stations. Therefore, improving both the density of the stations and the charging power can only lead to a slight saving in transportation costs. This finding can be of importance to the stakeholders (e.g., automakers and governments) in charge of investing in charging infrastructures. Since these infrastructures are often capital-intensive, there is no need to invest in both the charging technology and opening more charging stations to encourage delivery companies to use electric vehicles.

In addition, it has been observed that EVs are more likely to be employed for shorter distances. This implies that delivery companies may prefer to use EVs for shorter distances due to range anxiety. Although this is an intuitive finding, it sends an important message to the delivery companies who plan to utilize EVs for larger service areas to evaluate and ensure the accessibility of charging stations within their operating areas before any implementation.

Employing different solution methods, we found that the weighted-sum method had the best performance among all the presented multi-objective techniques. To gain insights into a real-world situation, we considered the case of Walmart Canada and the GTA. The results of the bi-objective model for different instance sets have been presented. We found that by increasing the number of stations and enhancing the power of the chargers, delivery companies that are using or plan to use heavy-duty electric trucks can lower their transportation costs and GHG emissions.

Furthermore, one interesting insight from our trade-off analysis is that by increasing a small amount of transportation costs, delivery companies can considerably reduce their GHG emissions. For the instances used in this study, considerable reductions in GHG emissions can occur because adding more EVs to the fleet may result in a slight rise in the costs but zero GHG emissions release. This finding could be important for delivery companies when the government provides some financial incentives to reduce emissions. Although government incentives to reduce emissions were not part of this study, this might be the case in practice. Therefore, such incentives can entirely cover the extra transportation costs when the emission is reduced.

Future research can examine the uncertainty in the parameters of this model, such as traveling time and energy consumption. These parameters can be handled by applying stochastic programming or robust optimization. In addition, the energy consumption model for EVs can be included in the mathematical model based on important factors such as the weight and speed of the vehicles, the characteristics of the roads, and even weather conditions. Lastly, exact solution methods such as branch-and-price and branch-and-cut methods can be combined with the multi-objective solution approaches to produce Pareto solutions.

CRediT authorship contribution statement

Afsane Amiri: Conceptualization, Methodology, Software, Validation, Writing – original draft, Writing – review & editing. **Saman Hassanzadeh Amin:** Funding acquisition, Conceptualization, Methodology, Software, Writing – original draft, Writing – review & editing, Supervision. **Hossein Zolfagharinia:** Funding acquisition, Conceptualization, Methodology, Software, Writing – original draft, Writing – review & editing, Supervision.

Declaration of Competing Interest

The authors declare the following financial interests/personal relationships which may be considered as potential competing interests: Saman Hassanzadeh Amin reports financial support was provided by Natural Sciences and Engineering Research Council of Canada. Hossein Zolfagharinia reports financial support was provided by Natural Sciences and Engineering Research Council of Canada.

Data availability

Data will be made available on request.

Acknowledgments

The authors would like to thank the editors and reviewers for the excellent comments that improved the quality of the paper significantly. This work was supported by Discovery Grants from the Natural Sciences and Engineering Research Council of Canada (grant# RGPIN-2017-04434 and grant# RGPIN-2017-04481).

References

Alabas-Uslu, C. (2008). A self-tuning heuristic for a multi-objective vehicle routing problem. *Journal of the Operational Research Society, 59*(7), 988–996.

Asghari, M., & Al-e, S. M. J. M. (2020). Green vehicle routing problem: A state-of-the-art review. *International Journal of Production Economics, 107899*.

Barth, M., Younglove, T., & Scora, G. (2005). Development of a Heavy-Duty Diesel Modal Emissions and Fuel Consumption Model. *UC Berkeley: California Partners for Advanced Transportation Technology*. Retrieved from https://escholarship.org/uc/item/67f0v3zf.

Braekers, K., Caris, A., & Janssens, G. K. (2011). A deterministic annealing algorithm for a bi-objective full truckload vehicle routing problem in drayage operations. *Procedia-Social and Behavioral Sciences, 20*, 344–353.

Bruglieri, M., Pezzella, F., Pisacane, O., & Suraci, S. (2015). A variable neighborhood search branching for the electric vehicle routing problem with time windows. *Electronic Notes in Discrete Mathematics, 47*, 221–228.

Bula, G. A., Afsar, H. M., González, F. A., Prodhon, C., & Velasco, N. (2019). Bi-objective vehicle routing problem for hazardous materials transportation. *Journal of Cleaner Production, 206*, 976–986.

CALSTART. (2020). *Drive to Zero's Zero-emission Technology Inventory (ZETI) Tool Version 5.9*. Retrieved from https://globaldrivetozero.org/tools/zero-emission-technology-inventory/. Accessed April 22, 2022.

Capuder, T., Sprčić, D. M., Zoričić, D., & Pandžić, H. (2020). Review of challenges and assessment of electric vehicles integration policy goals: Integrated risk analysis approach. *International Journal of Electrical Power & Energy Systems, 119*, Article 105894.

Caramia, M., & Dell'Olmo, P. (2020). Multi-objective optimization. In *Multi-objective management in freight logistics* (pp. 21–51). Cham: Springer.

Chen, C., Demir, E., & Huang, Y. (2021). An adaptive large neighborhood search heuristic for the vehicle routing problem with time windows and delivery robots. *European Journal of Operational Research, 294*(3), 1164–1180.

Conrad, R. G., & Figliozzi, M. A. (2011, May). The recharging vehicle routing problem. In *Proceedings of the 2011 industrial engineering research conference* (pp. 1-8).

Dabiri, N., Tarokh, M. J., & Alinaghian, M. (2017). New mathematical model for the bi-objective inventory routing problem with a step cost function: A multi-objective particle swarm optimization solution approach. *Applied Mathematical Modelling, 49*, 302–318.

Demir, E., Bektaş, T., & Laporte, G. (2014). The bi-objective pollution-routing problem. *European Journal of Operational Research, 232*(3), 464–478.

Desaulniers, G., Errico, F., Irnich, S., & Schneider, M. (2016). Exact algorithms for electric vehicle-routing problems with time windows. *Operations Research, 64*(6), 1388–1405.

Ding, N., Batta, R., & Kwon, C. (2015). *Conflict-free electric vehicle routing problem with capacitated charging stations and partial recharge* (pp. 1–24). Buffalo: SUNY.

Electric Autonomy. (2020). *Walmart places one of Canada's largest electric truck orders, 130 Tesla Semis*. Retrieved from https://electricautonomy.ca/2020/09/29/walmart-canada-electric-trucks/. Accessed April 22, 2022.

Electric Truck Guidance Report Series. (2020). *High-Potential Regions for Electric Truck Deployments*, Retrieved from https://nacfe.org/emerging-technology/electric-trucks/high-potential-regions-for-electric-truck-deployments/. Accessed April 22, 2022.

Electrify Canada. (2021). *Pricing and Plans for EV Charging*. Retrieved from https://www.electrify-canada.ca/. Accessed April 22, 2022.

Erdelić, T., & Carić, T. (2019). A survey on the electric vehicle routing problem: variants and solution approaches. *Journal of Advanced Transportation*, *2019*.

Erdoğan, S., & Miller-Hooks, E. (2012). A green vehicle routing problem. *Transportation Research Part E: Logistics and Transportation Review, 48*(1), 100–114.

Eskandarpour, M., Ouelhadj, D., Hatami, S., Juan, A. A., & Khosravi, B. (2019). Enhanced multi-directional local search for the bi-objective heterogeneous vehicle routing problem with multiple driving ranges. *European Journal of Operational Research, 277*(2), 479–491.

Felipe, Á., Ortuño, M. T., Righini, G., & Tirado, G. (2014). A heuristic approach for the green vehicle routing problem with multiple technologies and partial recharges. *Transportation Research Part E: Logistics and Transportation Review, 71*, 111–128.

Friedrich, C., & Elbert, R. (2022). Adaptive large neighborhood search for vehicle routing problems with transshipment facilities arising in city logistics. *Computers & Operations Research, 137*, Article 105491.

Froger, A., Mendoza, J. E., Jabali, O., & Laporte, G. (2017). A matheuristic for the electric vehicle routing problem with capacitated charging stations (Doctoral dissertation, Center interuniversitaire de recherche sur les reseaux d'entreprise, la logistique et le transport (CIRRELT)).

Froger, A., Mendoza, J. E., Jabali, O., & Laporte, G. (2019). Improved formulations and algorithmic components for the electric vehicle routing problem with nonlinear charging functions. *Computers & Operations Research, 104*, 256–294.

Garcia-Najera, A., & Bullinaria, J. A. (2011). An improved multi-objective evolutionary algorithm for the vehicle routing problem with time windows. *Computers & Operations Research, 38*(1), 287–300.

Ghoseiri, K., & Ghannadpour, S. F. (2010). Multi-objective vehicle routing problem with time windows using goal programming and genetic algorithm. *Applied Soft Computing, 10*(4), 1096–1107.

Goeke, D., & Schneider, M. (2015). Routing a mixed-fleet of electric and conventional vehicles. *European Journal of Operational Research, 245*(1), 81–99.

Gonçalves, F., Cardoso, S. R., Relvas, S., & Barbosa-Póvoa, A. P. F. D. (2011, April). Optimization of a distribution network using electric vehicles: A VRP problem. In *Proceedings of the IO2011-15 Congresso da associação Portuguesa de Investigação Operacional, Coimbra, Portugal* (pp. 18-20).

Government of Canada. (2021a). *Canadian Environmental Sustainability Indicators: Greenhouse gas emissions*. Retrieved from https://www.canada.ca/en/environment-climate-change/services/environmental-indicators/greenhouse-gas-emissions.html. Accessed April 22, 2022.

Government of Canada. (2021b). Discussion paper on heavy-duty vehicles and engines in Canada: transitioning to a zero-emission future. Retrieved from https://www.canada.ca/en/environment-climate-change/services/canadian-environmental-protection-act-registry/heavy-duty-vehicle-engines-zero-emission-future-discussion-paper.html. Accessed April 22, 2022.

Government of Canada. (2021c). *Zero Emission Vehicle Infrastructure Program*. Retrieved from https://www.nrcan.gc.ca/energy-efficiency/transportation-alternative-fuels/zero-emission-vehicle-infrastructure-program/21876. Accessed April 22, 2022.

Green Car Congress. (2018). *Walmart Canada commits to 100% alternatively powered fleet vehicles by 2028; orders 30 more Tesla semis*. Retrieved from https://www.greencarcongress.com/2018/09/20180909-walmart.html. Accessed April 22, 2022.

Green Car Reports. (2017). *Wal-Mart, Anheuser-Busch, DHL to test Tesla Semi; now UPS, Pepsi too (more updates)*. Retrieved from https://www.greencarreports.com/news/1114246_wal-mart-anheuser-busch-dhl-to-test-tesla-semi-1200-plus-reservations. Accessed April 22, 2022.

Guerriero, F., Surace, R., Loscri, V., & Natalizio, E. (2014). A multi-objective approach for unmanned aerial vehicle routing problem with soft time windows constraints. *Applied Mathematical Modelling, 38*(3), 839–852.

Guidance Report: Viable Class 7/8 Electric, Hybrid and Alternative Fuel Tractors. (2019). Retrieved from https://nacfe.org/emerging-technology/electric-trucks-2/viable-class-7-8/. Accessed April 22, 2022.

Hiermann, G., Puchinger, J., Ropke, S., & Hartl, R. F. (2016). The electric fleet size and mix vehicle routing problem with time windows and recharging stations. *European Journal of Operational Research, 252*(3), 995–1018.

Hulagu, S., Atasayar, G., & Celikoglu, H. B. (2019, September). Green routing plan for university shuttle services using mixed integer linear programming. In *2019 IEEE 5th International forum on Research and Technology for Society and Industry (RTSI)* (pp. 471-476). IEEE.

Kancharla, S. R., & Ramadurai, G. (2018). An adaptive large neighborhood search approach for electric vehicle routing with load-dependent energy consumption. *Transportation in Developing Economies, 4*(2), 1–9.

Keskin, M., & Çatay, B. (2016). Partial recharge strategies for the electric vehicle routing problem with time windows. *Transportation Research Part C: Emerging Technologies, 65*, 111–127.

Keskin, M., & Çatay, B. (2018). A matheuristic method for the electric vehicle routing problem with time windows and fast chargers. *Computers & Operations Research, 100*, 172–188.

Keskin, M., Laporte, G., & Çatay, B. (2019). Electric Vehicle Routing Problem with Time-Dependent Waiting Times at Recharging Stations. *Computers & Operations Research, 107*, 77–94.

Kim, I. Y., & De Weck, O. L. (2005). Adaptive weighted-sum method for bi-objective optimization: Pareto front generation. *Structural and multidisciplinary optimization, 29*(2), 149–158.

Koç, Ç., & Karaoglan, I. (2016). The green vehicle routing problem: A heuristic based exact solution approach. *Applied Soft Computing, 39*, 154–164.

Koç, Ç., Jabali, O., Mendoza, J. E., & Laporte, G. (2019). The electric vehicle routing problem with shared charging stations. *International Transactions in Operational Research, 26*(4), 1211–1243.

Kullman, N., Goodson, J., Mendoza, J.E. (2020). Electric Vehicle Routing with Public Charging Stations. ⟨hal-01928730v2⟩.

Kyriakakis, N. A., Sevastopoulos, I., Marinaki, M., & Marinakis, Y. (2022). A hybrid Tabu search–Variable neighborhood descent algorithm for the cumulative capacitated vehicle routing problem with time windows in humanitarian applications. *Computers & Industrial Engineering, 164*, Article 107868.

Lee, C. (2020). An exact algorithm for the electric-vehicle routing problem with nonlinear charging time. *Journal of the Operational Research Society*, 1–24.

Leggieri, V., & Haouari, M. (2017). A practical solution approach for the green vehicle routing problem. *Transportation Research Part E: Logistics and Transportation Review, 104*, 97–112.

Li, X., Shi, X., Zhao, Y., Liang, H., & Dong, Y. (2020). SVND enhanced metaheuristic for plug-in hybrid electric vehicle routing problem. *Applied Sciences, 10*(2), 441.

Liimatainen, H., van Vliet, O., & Aplyn, D. (2019). The potential of electric trucks–An international commodity-level analysis. *Applied energy, 236*, 804–814.

Macrina, G., Pugliese, L. D. P., Guerriero, F., & Laporte, G. (2019). The green mixed fleet vehicle routing problem with partial battery recharging and time windows. *Computers & Operations Research, 101*, 183–199.

Macrina, G., Laporte, G., Guerriero, F., & Pugliese, L. D. P. (2019). An energy-efficient green-vehicle routing problem with mixed vehicle fleet, partial battery recharging and time windows. *European Journal of Operational Research, 276*, 971–982.

Marler, R. T., & Arora, J. S. (2004). Survey of multi-objective optimization methods for engineering. *Structural and multidisciplinary optimization, 26*(6), 369–395.

Marler, R. T., & Arora, J. S. (2010). The weighted sum method for multi-objective optimization: New insights. *Structural and multidisciplinary optimization, 41*(6), 853–862.

Mavrotas, G. (2009). Effective implementation of the ε-constraint method in multi-objective mathematical programming problems. *Applied mathematics and computation, 213*(2), 455–465.

Mavrotas, G., & Florios, K. (2013). An improved version of the augmented ε-constraint method (AUGMECON2) for finding the exact pareto set in multi-objective integer programming problems. *Applied Mathematics and Computation, 219*(18), 9652–9669.

Máximo, V. R., Cordeau, J. F., & Nascimento, M. C. (2022). An adaptive iterated local search heuristic for the Heterogeneous Fleet Vehicle Routing Problem. *Computers & Operations Research, 148*, Article 105954.

Máximo, V. R., & Nascimento, M. C. (2021). A hybrid adaptive iterated local search with diversification control to the capacitated vehicle routing problem. *European Journal of Operational Research, 294*(3), 1108–1119.

MBA Knowledge Base. (2022). *Case Study: Wal-Mart's Distribution and Logistics System*. Retrieved from https://www.mbaknol.com/management-case-studies/case-study-of-walmart-logistics-management/. Accessed April 22, 2022.

Melián-Batista, B., De Santiago, A., AngelBello, F., & Alvarez, A. (2014). A bi-objective vehicle routing problem with time windows: A real case in Tenerife. *Applied Soft Computing, 17*, 140–152.

Montoya, A., Guéret, C., Mendoza, J. E., & Villegas, J. G. (2016). A multi-space sampling heuristic for the green vehicle routing problem. *Transportation Research Part C: Emerging Technologies, 70*, 113–128.

Montoya, A., Guéret, C., Mendoza, J. E., & Villegas, J. G. (2017). The electric vehicle routing problem with nonlinear charging function. *Transportation Research Part B: Methodological, 103*, 87–110.

Pan-Canadian Framework on Clean Growth and Climate Change. (2016). Retrieved from http://publications.gc.ca/site/eng/9.828774/publication.html. Accessed April 22, 2022.

Parastvand, H., Moghaddam, V., Bass, O., Masoum, M. A., Chapman, A., & Lachowicz, S. (2020). A graph automorphic approach for placement and sizing of charging stations in EV network considering traffic. *IEEE Transactions on Smart Grid, 11*(5), 4190–4200.

Pelletier, S., Jabali, O., & Laporte, G. (2016). 50th anniversary invited article—goods distribution with electric vehicles: Review and research perspectives. *Transportation Science, 50*(1), 3–22.

Pisinger, D., & Ropke, S. (2007). A general heuristic for vehicle routing problems. *Computers & operations research, 34*(8), 2403–2435.

Plug 'n Drive. (2021). Retrieved from https://www.plugndrive.ca/electric-vehicle-range/?gclid=Cj0KCQiA_c-OBhDFARIsAIFg3eyyNVsw9Iu36LAEXARXxEbtn227qddlITcHP4BP_fY56T2DkzuQkWMaAuS3EALw_wcB. Accessed April 22, 2022.
Puls News. (2022). *Walmart's New FAST Unloader Shows Intelligence of Motor-Driven Roller Conveyors*. Retrieved from https://www.pulseroller.com/resources/pulsenews/walmart_s_new_fast_unloader_shows_intelligence_of_motor_driven_roller_conveyors. Accessed April 22, 2022.
Ren, X., Huang, H., Feng, S., & Liang, G. (2020). An improved variable neighborhood search for bi-objective mixed-energy fleet vehicle routing problem. *Journal of Cleaner Production, 275*, Article 124155.
Ropke, S., & Pisinger, D. (2006). An adaptive large neighborhood search heuristic for the pickup and delivery problem with time windows. *Transportation science, 40*(4), 455–472.
Sassi, O., Cherif, W. R., & Oulamara, A. (2014). Vehicle routing problem with mixed fleet of conventional and heterogenous electric vehicles and time dependent charging costs. ⟨hal-01083966⟩.
Sassi, O., Cherif-Khettaf, W. R., & Oulamara, A. (2015). Iterated tabu search for the mix fleet vehicle routing problem with heterogenous electric vehicles. In *Modelling, Computation and Optimization in Information Systems and Management Sciences* (pp. 57–68). Cham: Springer.
Sassi, O., Cherif-Khettaf, W. R., & Oulamara, A. (2015, April). Multi-start iterated local search for the mixed fleet vehicle routing problem with heterogenous electric vehicles. In *European Conference on Evolutionary Computation in Combinatorial Optimization* (pp. 138–149). Cham: Springer.
Schneider, M., Stenger, A., & Goeke, D. (2014). The electric vehicle-routing problem with time windows and recharging stations. *Transportation Science, 48*(4), 500–520.
Schoenberg, S., & Dressler, F. (2022). Reducing Waiting Times at Charging Stations with Adaptive Electric Vehicle Route Planning. *IEEE Transactions on Intelligent Vehicles.*
Shukla, A., Verma, K., & Kumar, R. (2019). Multi-objective synergistic planning of EV fast-charging stations in the distribution system coupled with the transportation network. *IET Generation, Transmission & Distribution, 13*(15), 3421–3432.
Sripad, S., & Viswanathan, V. (2017). Performance metrics required of next-generation batteries to make a practical electric semi truck. *ACS Energy Letters, 2*(7), 1669–1673.
Supermarket News (2021). *Walmart to build first Atlantic Canada distribution center*. Retrieved from https://www.supermarketnews.com/retail-financial/walmart-build-first-atlantic-canada-distribution-center. Accessed April 22, 2022.
Talk Business & Politics (2018). *Walmart tests FAST unloader in 30 of its busiest supercenters*. Retrieved from https://talkbusiness.net/2018/06/walmart-tests-fast-unloader-in-30-of-its-busiest-supercenters/. Accessed April 22, 2022.
TESMANIAN (2020). *Tesla Semi's <2kWh/mile Consumption Hints at Serious Battery Improvements and Cost Reduction*. Retrieved from https://www.tesmanian.com/blogs/tesmanian-blog/tesla-semi-page-update-hints-at-massive-battery-improvements-and-cost-reduction. Accessed April 22, 2022.
Tirkolaee, E. B., Goli, A., Gütmen, S., Weber, G. W., & Szwedzka, K. (2022). A novel model for sustainable waste collection arc routing problem: Pareto-based algorithms. *Annals of Operations Research*, 1–26.
Transportation Association of Canada. (2017). Geometric design guide for Canadian roads. Ottawa.
Truck News. (2021). *Hydro One's heavy-duty truck charging pilot included in new EV funds*. Retrieved from https://www.trucknews.com/equipment/hydro-ones-heavy-duty-truck-charging-pilot-included-in-new-ev-funds/1003152578/. Accessed April 22, 2022.
Trucks.com. (2019). *Here's Everything We Know About the Tesla Semi*. Retrieved from https://www.trucks.com/2019/09/05/everything-we-know-about-the-tesla-semi-truck/. Accessed April 22, 2022.
Villegas, J. G., Guéret, C., Mendoza, J. E., & Montoya, A. (2018). The technician routing and scheduling problem with conventional and electric vehicle. In *Technical Report.*
Vincent, F. Y., Jodiawan, P., & Gunawan, A. (2021). An Adaptive Large Neighborhood Search for the green mixed fleet vehicle routing problem with realistic energy consumption and partial recharges. *Applied Soft Computing, 105*, Article 107251.
Voigt, S., Frank, M., Fontaine, P., & Kuhn, H. (2022). Hybrid Large Neighborhood Search for the Capacitated Vehicle Routing Problem and the Vehicle Routing Problem with Time Windows. *Available at SSRN 4176106*.
Walmart. (2021). Retrieved from https://www.walmart.ca/en/stores-near-me. Accessed April 22, 2022.
Walmart Canada. (2021). *Logistics*. Retrieved from https://www.walmartcanada.ca/our-story/our-business. Accessed April 22, 2022.
Walmart Canada Corp. (2021). *Walmart Canada unveils state-of-the-art warehouse technology in Cornwall, Ontario*. Retrieved from https://www.newswire.ca/news-releases/walmart-canada-unveils-state-of-the-art-warehouse-technology-in-cornwall-ontario-885743190.html. Accessed April 22, 2022.
Wang, R., Zhou, Z., Ishibuchi, H., Liao, T., & Zhang, T. (2016). Localized weighted sum method for many-objective optimization. *IEEE Transactions on Evolutionary Computation, 22*(1), 3–18.
Yang, G., Xu, H., Wang, Z., & Tian, Z. (2016). Truck acceleration behavior study and acceleration lane length recommendations for metered on-ramps. *International Journal of Transportation Science and Technology, 5*(2), 93–102.
Yang, S., Ning, L., Tong, L. C., & Shang, P. (2021). Optimizing electric vehicle routing problems with mixed backhauls and recharging strategies in multi-dimensional representation network. *Expert Systems with Applications, 176*, Article 114804.
Yu, H., & Solvang, W. D. (2016). An improved multi-objective programming with augmented ε-constraint method for hazardous waste location-routing problems. *International Journal of Environmental Research and Public Health, 13*(6), 548.
Zajac, S., & Huber, S. (2021). Objectives and methods in multi-objective routing problems: A survey and classification scheme. *European Journal of Operational Research, 290*(1), 1–25.
Zarouk, Y., Mahdavi, I., Rezaeian, J., & Santos-Arteaga, F. J. (2022). A novel multi-objective green vehicle routing and scheduling model with stochastic demand, supply, and variable travel times. *Computers & Operations Research, 141*, Article 105698.
Zhang, H., Zhang, Q., Ma, L., Zhang, Z., & Liu, Y. (2019). A hybrid ant colony optimization algorithm for a multi-objective vehicle routing problem with flexible time windows. *Information Sciences, 490*, 166–190.
Zhang, S., Gajpal, Y., Appadoo, S. S., & Abdulkader, M. M. S. (2018). Electric vehicle routing problem with recharging stations for minimizing energy consumption. *International Journal of Production Economics, 203*, 404–413.
Zitzler, E., & Thiele, L. (1998). An evolutionary algorithm for multiobjective optimization: The strength pareto approach. *TIK-report, 43*.
Zitzler, E., Thiele, L., Laumanns, M., Fonseca, C. M., & Da Fonseca, V. G. (2003). Performance assessment of multiobjective optimizers: An analysis and review. *IEEE Transactions on evolutionary computation, 7*(2), 117–132.
Zolfagharinia, H., & Haughton, M. (2017). Operational flexibility in the truckload trucking industry. *Transportation Research Part B: Methodological, 104*, 437–460.
Zolfagharinia, H., & Haughton, M. (2018). The importance of considering non-linear layover and delay costs for local truckers. *Transportation Research Part E: Logistics and Transportation Review, 109*, 331–355.
Zuo, X., Xiao, Y., You, M., Kaku, I., & Xu, Y. (2019). A new formulation of the electric vehicle routing problem with time windows considering concave nonlinear charging function. *Journal of Cleaner Production, 236*, Article 117687.